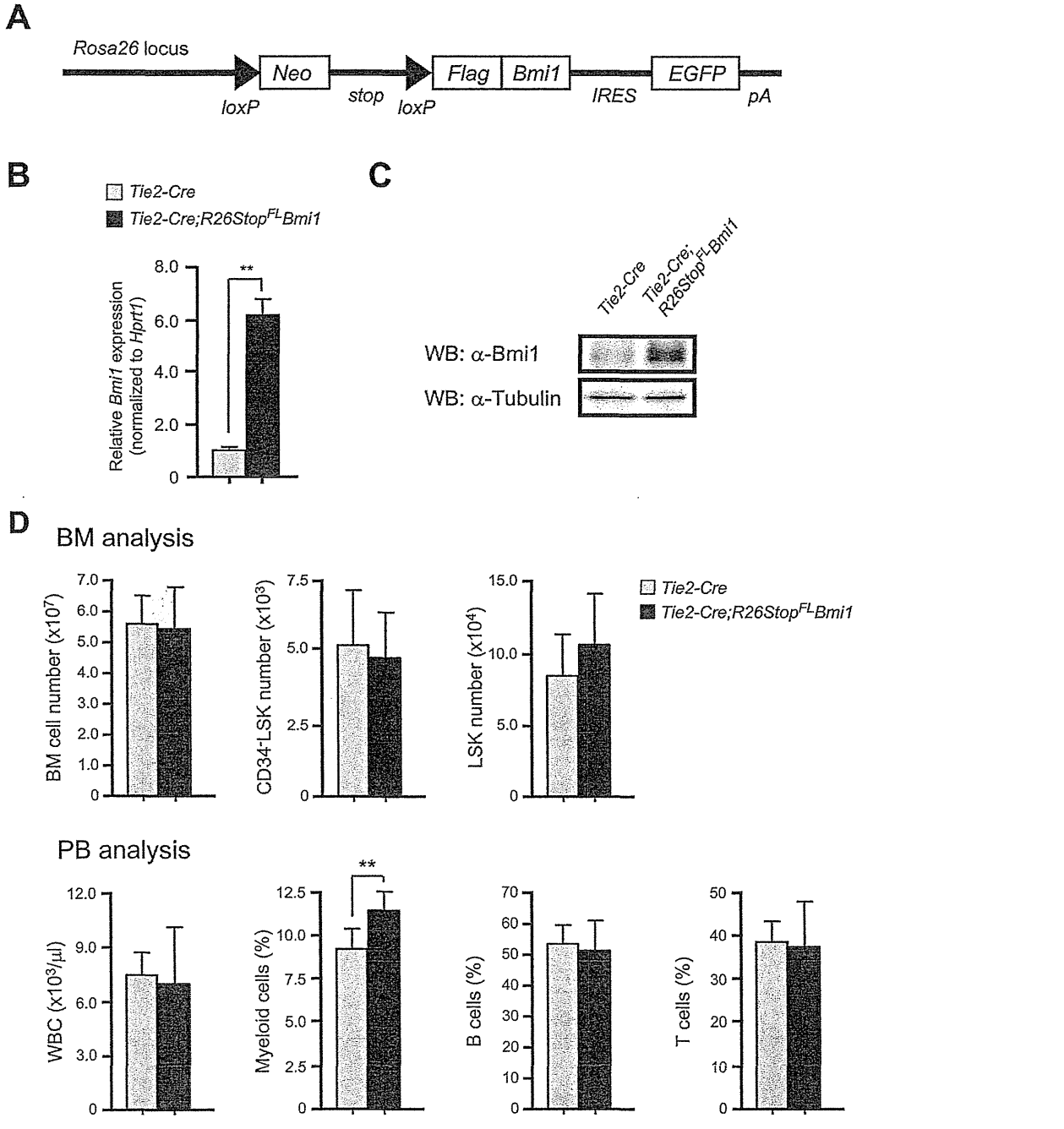

Figure 1. Generation of mice overexpressing *Bmi1* in hematopoietic cells. (A) Strategy for making a knock-in allele for *Bmi1* downstream of the *Rosa26* promoter. A *loxP*-flanked *neo*^{r}-stop cassette followed by Flag-tagged *Bmi1*, an *frt*-flanked *IRES-eGFP* cassette, and a bovine polyadenylation sequence was knocked-in the *Rosa26* locus. (B) Quantitative RT-PCR analysis of *Bmi1* in BM LSK cells from *Tie2-Cre* and *Tie2-Cre;R26Stop*^{FL}*Bmi1* mice. mRNA levels were normalized to *Hprt1* expression. Expression levels relative to that in *Tie2-Cre* LSK cells are shown as the mean ± S.D. (n = 3). (C) Western blotting analysis of Bmi1 in c-Kit$^+$ BM cells from *Tie2-Cre* and *Tie2-Cre;R26Stop*^{FL}*Bmi1* mice. α-tubulin was used as the loading control. (D) Hematopoietic analysis of 10-week-old *Tie2-Cre* and *Tie2-Cre;R26Stop*^{FL}*Bmi1* mice. Absolute numbers of BM cells, CD34$^-$LSK cells, and LSK cells in bilateral femurs and tibiae are presented as the mean ± S.D. (upper panels, *Tie2-Cre*; n = 7, *Tie2-Cre;R26Stop*^{FL}*Bmi1*; n = 8). PB analysis of 10-week-old *Tie2-Cre* and *Tie2-Cre;R26Stop*^{FL}*Bmi1* mice. White blood cell (WBC) counts and lineage contribution of myeloid, B, and T cells are shown as the mean ± S.D. (lower panels, *Tie2-Cre*; n = 7, *Tie2-Cre;R26Stop*^{FL}*Bmi1*; n = 8). ** $p<0.01$.
doi:10.1371/journal.pone.0036209.g001

HSCs are exposed to various stresses including replicative and oxidative stresses during serial transplantation and eventually lose self-renewal capacity [16,17]. We hypothesized that the effects of overexpression of *Bmi1* on HSCs would manifest under stressful conditions such as serial transplantations. Therefore, we performed competitive repopulation assays using 5×10^5 fresh BM

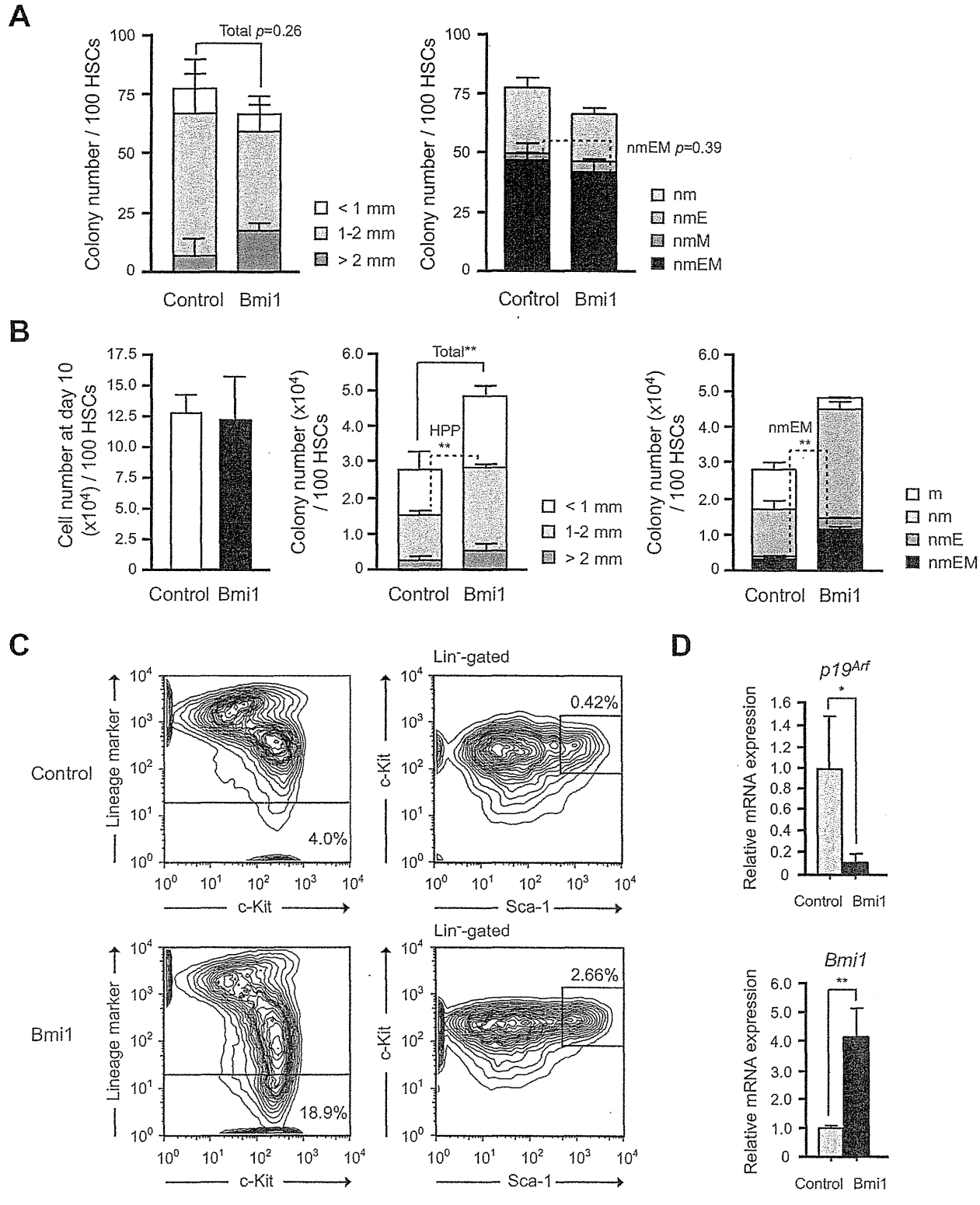

Figure 2. Effects of overexpression of *Bmi1* on HSCs *in vitro*. (A) Colony formation by HSCs isolated from *Tie2-Cre* (Control) and *Tie2-Cre;R26Stop^{FL}Bmi1* (Bmi1) mice. Single CD34$^-$LSK cells were sorted into 96-well microtiter plates containing the SF-O3 medium supplemented with 10% FBS and multiple cytokines (10 ng/ml SCF, 10 ng/ml TPO, 10 ng/ml IL-3, and 3 u/ml EPO) and allowed to form colonies. At day 14 of culture, the colonies were counted and individually collected for morphological examination. Absolute numbers of LPP and HPP-CFCs which gave rise to colonies with a diameter less and greater than 1 mm, respectively are shown as the mean ± S.D. for triplicate cultures (left panel). Absolute numbers of each

colony types were defined by the composition of colonies (right panel). Colonies were recovered and examined by microscopy to determine colony types. Composition of colonies is depicted as n, neutrophils; m, macrophages; E, erythroblasts; and M, megakaryocytes. (B) Colony formation by HSCs cultured for 10 days. $CD34^-LSK$ cells from *Tie2-Cre* (Control) and *Tie2-Cre;R26Stop^{FL}Bmi1* (Bmi1) mice were cultured in the SF-O3 serum-free medium supplemented with 50 ng/ml of SCF and TPO. At day 10 of culture, the cells were counted (left panel) and plated in methylcellulose medium to allow formation of colonies in the presence of 20 ng/ml SCF, 20 ng/ml TPO, 20 ng/ml IL-3, and 3 u/ml EPO. Absolute numbers of LPP and HPP-CFCs (middle panel) are shown as the mean ± S.D. for triplicate cultures. Absolute numbers of each colony type are shown in the right panel. (C) Flow cytometric analysis of $CD34^-LSK$ HSCs at day14 of culture. Representative flow cytometric profiles of LSK cells in cultures of $CD34^-LSK$ HSCs from *Tie2-Cre* (Control) and *Tie2-Cre;R26Stop^{FL}Bmi1* (Bmi1) mice are depicted. The proportion of Lin^- and LSK cells in total cells are indicated. (D) Quantitative RT-PCR analysis of the expression of *p19^{Arf}*, and *Bmi1* in *Tie2-Cre* (Control) and *Tie2-Cre;R26Stop^{FL}Bmi1* (Bmi1) LSK cells. LSK cells were purified by cell sorting from $CD34^-LSK$ cultures in (C) at day 14 of culture. Each value was normalized to *Hprt1* expression and the expression level of each gene in control cells was arbitrarily set to 1. Data are shown as the mean ± S.D. for triplicate analyses. * $p<0.05$, ** $p<0.01$.
doi:10.1371/journal.pone.0036209.g002

cells along with 5×10^5 competitor BM cells (**Figure 4A**) or the total cells produced from 20 $CD34^-LSK$ cells after a 10-day culture period along with 2×10^5 competitor BM cells (**Figure 4B**). The flow cytometric analysis of PB revealed little or no difference in the chimerism of donor cells between *Tie2-Cre* and *Tie2-Cre;R26Stop^{FL}Bmi1* cells at 12 weeks after the primary transplantations. However, in the secondary and tertiary transplantations, the chimerism of *Tie2-Cre* cells significantly declined while that of *Tie2-Cre;R26Stop^{FL}Bmi1* cells drasticaly increased. *Tie2-Cre* cells after 10-day culture failed to reconstitute hematopoiesis in the quaternary transplantation, while *Tie2-Cre;R26Stop^{FL}Bmi1* cells still established robust repopulation (**Figure 4B**). The chimerism of donor cells in BM LSK cells mirrored the changes in the PB. These results clearly indicate that overexpression of *Bmi1* protects HSCs against the loss of self-renewal capacity during serial transplantation. The findings thus far suggest that overexpression of *Bmi1* confers stress resistance onto HSCs.

Summary of % of engrafted mice and frequency of HSCs in CRU assays

	Number of $CD34^-LSK$ cells injected							Frequency		95% CI
	0.5	1	1.5	2	5	10	20			
Fresh control				1/9	4/10	7/10	6/6	1/8		1/14~1/5
Fresh Bmi1				1/10	6/10	6/10	5/5	1/8		1/13~1/5
Cultured control	1/7	4/7	3/8	7/10	10/10	9/9		1/2	***	1/3~1/1
Cultured Bmi1	5/7	6/7	8/8	8/10	9/10	10/10		1/1	***	1/2~1/1

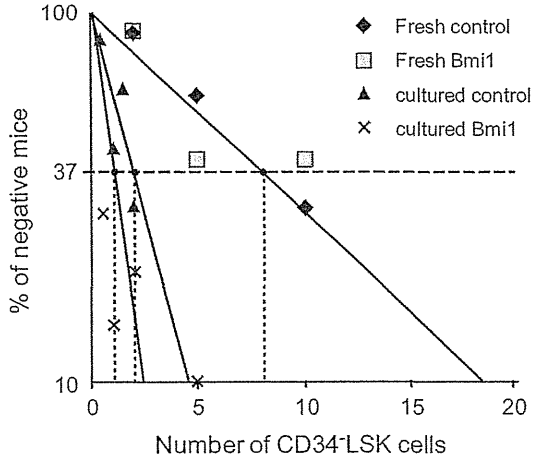

Figure 3. Overexpression of *Bmi1* enhances expansion of HSCs *ex vivo*. Competitive repopulating unit (CRU) assays using limiting numbers of $CD34^-LSK$ cells from *Tie2-Cre* (Control) mice and *Tie2-Cre;R26Stop^{FL}Bmi1* (Bmi1) mice. Freshly isolated $CD34^-LSK$ cells were immediately used for BM transplantation, or $CD34^-LSK$ cells were cultured in the SF-O3 serum-free medium supplemented with 50 ng/ml SCF and TPO for 10 days, and then a fraction of the culture cells corresponding to the indicated number (0.5~10) of initial $CD34^-LSK$ cells was subjected to BM transplantation. The test cells (CD45.2) were transplanted along with 2×10^5 competitor BM cells (CD45.1) into CD45.1 recipient mice lethally irradiated at a dose of 9.5 Gy. Percent chimerism of donor cells in the recipient PB was determined at 16 weeks after transplantation. The mice with chimerism more than 1% in all three lineages (myeloid, B, and T cells) were considered successfully engrafted and the others were defined as negative mice. The frequency of HSCs was calculated using L-Calc software. The proportion of engrafted mice, frequency of functional HSCs, and the 95% confidence interval (CI) are summarized in the table and each data is plotted in the bottom panel. *** $p<0.001$.
doi:10.1371/journal.pone.0036209.g003

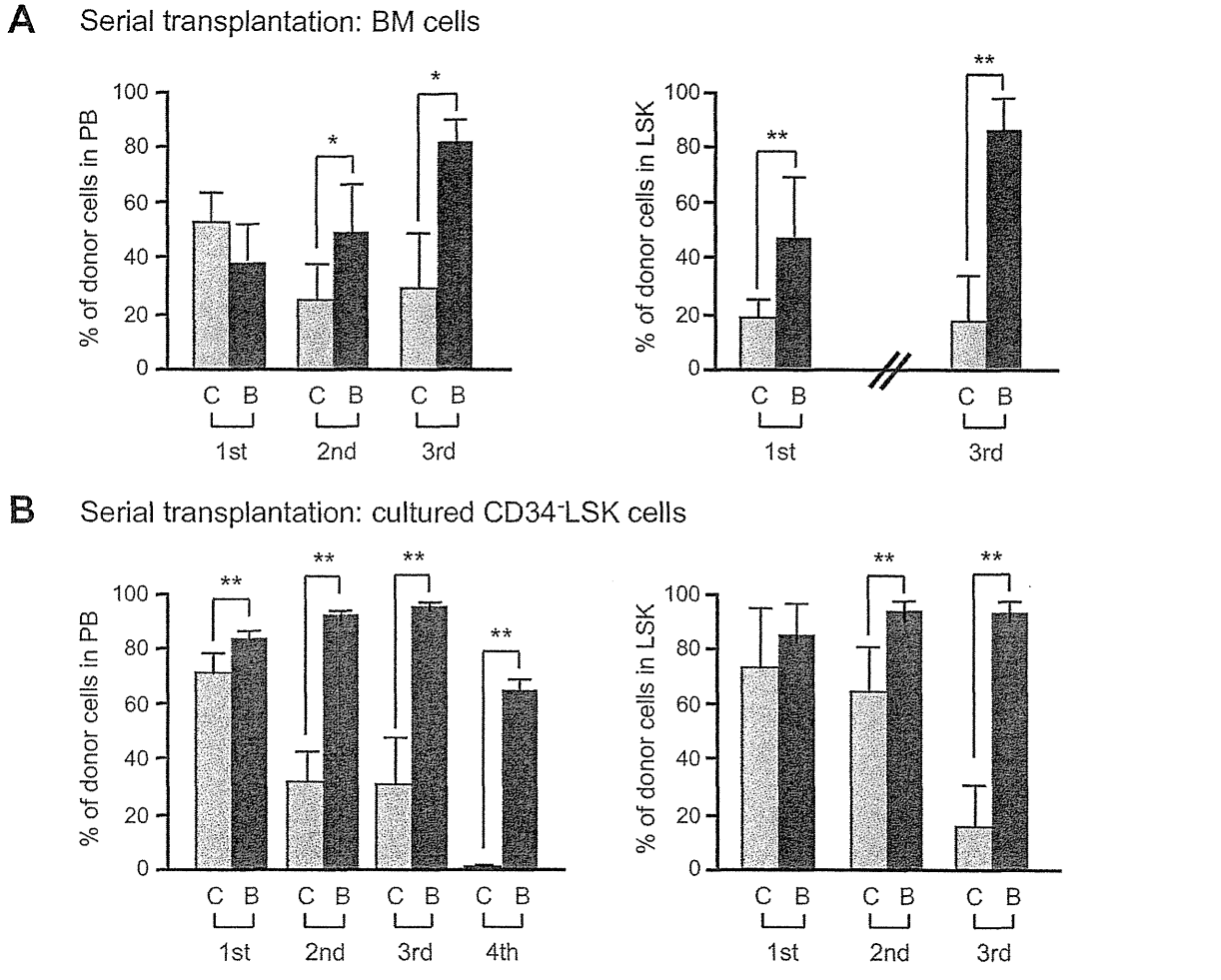

Figure 4. Overexpression of *Bmi1* protects HSCs during serial transplantation. (A) Serial transplantation of BM cells. BM cells (5×10^5) from *Tie2-Cre* (denoted as "C") and *Tie2-Cre;R26Stop^{FL}Bmi1* (denoted as "B") mice (CD45.2) along with 5×10^5 competitor BM cells (CD45.2) were transplanted into CD45.1 recipient mice lethally irradiated at a dose of 9.5 Gy. For serial transplantation, BM cells were collected from all recipient mice at 12–20 weeks after transplantation and pooled together. Then, 5×10^6 BM cells were transplanted into lethally irradiated recipient mice without competitor cells. Third and fourth transplantation were similarly performed using 5×10^6 pooled BM cells. Percent chimerism of donor cells in the recipient PB and BM LSK cells was determined at 16 weeks post-transplantation. Results are shown as the mean ± S.D. (n = 6, 3rd transplantation; n = 4). (B) Serial transplantation of cultured CD34$^-$LSK cells. CD34$^-$LSK cells were cultured in the SF-O3 serum-free medium supplemented with 50 ng/ml of SCF and TPO for 10 days. Then, the cells in culture corresponding to the 20 initial CD34$^-$LSK cells were injected into a recipient mouse along with 2×10^5 competitor BM cells (CD45.2) as described in (A) (n = 6, 4th transplantation; n = 5). * $P<0.05$, ** $P<0.01$.
doi:10.1371/journal.pone.0036209.g004

Overexpression of *Bmi1* has no Impact on Radioprotection

DNA damage is intimately linked to stem cell aging. Heritable DNA damage accrued in stem cells leads to stem cell senescence or apoptosis, which over time can lead to the depletion of the stem cell pool and reduced regenerative capacity of stem cells [18]. Bmi1 is rapidly recruited to sites of DNA damage and is required for DNA damage-induced ubiquitination of histone H2A at lysine 119. Loss of Bmi1 leads to impaired repair of DNA double-strand breaks (DSBs) by homologous recombination [19,20]. In glioblastoma multiforme (GBM) cells, Bmi1 was co-purified with DSB response proteins, such as ATM and the histone γH2AX, and non-homologous end joining (NHEJ) repair proteins. Of interest, BMI1 overexpression in normal neural stem cells enhanced ATM recruitment to the chromatin, the rate of γH2AX foci resolution, and resistance to radiation [21]. In order to understand the role of overexpressed Bmi1 in HSCs, we examined the radioresistance of HSCs by quantifying the number of γH2AX foci following genotoxic stress, a metric which reflects DNA DSBs.

We purified CD34$^-$LSK cells from *Tie2-Cre* and *Tie2-Cre;R26-Stop^{FL}Bmi1* mice and irradiated them at a dose of 2 Gy. At 2 and 4 hours after irradiation, cells were stained with anti-γH2AX. We expected rapid resolution of γH2AX by overexpression of *Bmi1*, but no significant difference was observed in the number of γH2AX foci between *Tie2-Cre* and *Tie2-Cre;R26Stop^{FL}Bmi1* HSCs (**Figure 5A**). HSCs recovered from the recipients of tertiary transplantation did not show any difference in the number of γH2AX foci, either (**Figure 5B**). We then tested hematopoietic recovery after irradiation in mice. We irradiated recipient mice reconstituted with *Tie2-Cre* and *Tie2-Cre;R26Stop^{FL}Bmi1* BM cells at a dose of 5 Gy, and monitored hematopoietic recovery for 4 weeks. The recovery of hematopoietic components in PB as well as

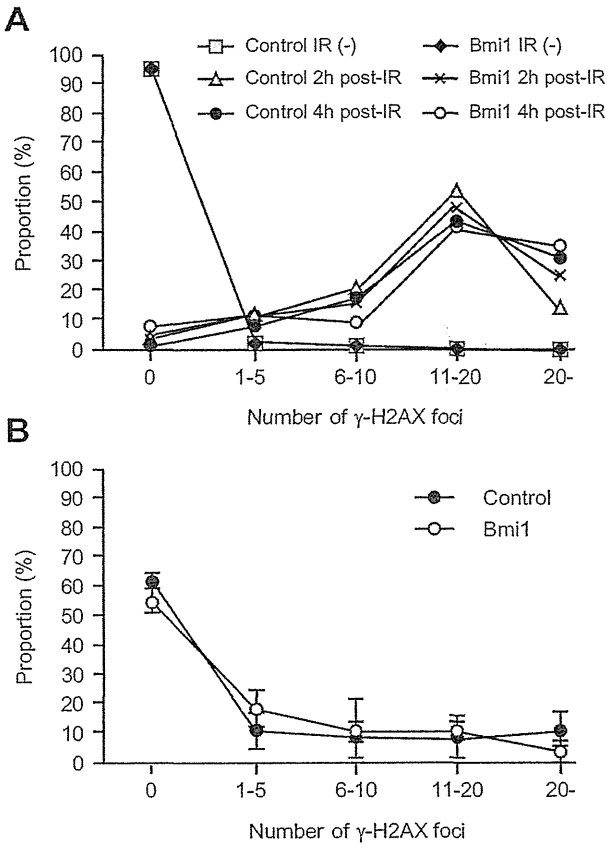

Figure 5. DNA damage response of *Tie2-Cre;R26Stop^{FL}Bmi1* HSCs. (A) DNA damage response of CD34$^-$LSK cells from *Tie2-Cre* (Control) and *Tie2-Cre;R26Stop^{FL}Bmi1* (Bmi1) mice *in vitro*. Purified CD34$^-$LSK cells were irradiated (IR) at a dose of 2 Gy. At 2 and 4 hours after irradiation, cells were stained with anti-γH2AX. Numbers of γH2AX foci expressed per cell are depicted. (B) DNA damage response of CD34$^-$LSK cells from *Tie2-Cre* (Control) and *Tie2-Cre;R26Stop^{FL}Bmi1* (Bmi1) mice *in vivo*. LSK cells were purified from the recipients of tertiary transplantation and stained with anti-γH2AX. Numbers of γH2AX foci expressed per cell are depicted as the mean ± S.D. (n = 3).
doi:10.1371/journal.pone.0036209.g005

BM LSK cells was comparable between the two groups (**Figure S3**). These findings suggest that overexpression of *Bmi1* does not afford an advantage to HSCs in their ability to resist genotoxic stress.

Overexpression of *Bmi1* Confers Resistance to Oxidative Stress on HSCs

HSCs contain lower levels of reactive oxygen species (ROS) than their mature progeny in order to maintain their quiescent state. ROS reportedly act through p38 mitogen-activated protein kinase (MAPK) to limit the lifespan of HSCs [16,22]. It has been demonstrated that prolonged treatment with the antioxidant *N*-acetyl-L-cysteine (NAC) or an inhibitor of p38 MAPK extends the lifespan of HSCs in serial transplantation assays, suggesting that oxidative stress is one of the major factors that affects HSC function during these assays [16,17,23]. Given that *Tie2-Cre;R26-Stop^{FL}Bmi1* HSCs retain self-renewal capacity during serial transplantation, overexpression of *Bmi1* may bestow a protective effect onto HSCs against oxidative stress.

To address this question, we cultured HSCs in the presence of buthionine sulfoximine (BSO), which depletes intracellular glutathione and thereby increases intracellular ROS levels. We found that highly purified CD34$^-$LSK HSCs were susceptible to an increase in ROS levels because treatment with BSO significantly suppressed their growth and induced cell death (data not shown). After 3 days of BSO treatment, surviving cells were subjected to colony-forming assays. Both *Tie2-Cre* control and *Tie2-Cre;R26-Stop^{FL}Bmi1* HSCs cultured with BSO gave rise to significantly fewer colonies than HSCs cultured without BSO. Interestingly, *Tie2-Cre;R26Stop^{FL}Bmi1* HSCs gave rise to a significantly more colonies than the control HSCs (**Figure 6A**). Notably, the number of HPP colonies was reduced 48-fold after treatment of control HSCs with BSO, but only 3-fold upon overexpression of *Bmi1*. The frequency of CFU-nmEM was also less perturbed following treatment with BSO in HSCs overexpressing *Bmi1*. These results indicate a role for Bmi1 in the resistance to oxidative stress.

Bmi1 regulates mitochondrial function by regulating the expression of a cohort of genes related to mitochondrial function and ROS generation. *Bmi1*-deficient cells have impaired mitochondrial function, which causes a marked increase in the intracellular levels of ROS [24]. Based on these observations, we then measured the intracellular ROS levels in CD34$^-$LSK cells at day 14 of culture. Unexpectedly, overexpression of *Bmi1* did not affect the levels of ROS in either LSK HSCs/MPPs or Lin$^-$Sca-1$^{low/-}$c-Kit$^+$ downstream progenitors (**Figure 6B**). Overexpression of *Bmi1* had no significant effect on the ROS levels even in the presence of BSO (**Figure S4**). Likewise, treatment of cells with the antioxidant NAC promoted cell growth and increased the proportion of LSK cells in both control and *Tie2-Cre;R26-Stop^{FL}Bmi1* culture similarly (**Figure 6C** and data not shown). These results indicate that an excess of Bmi1 does not regulate the generation or scavenging of ROS, but confers resistance to higher levels of ROS on HSCs through unknown mechanisms.

Discussion

In this study, we generated a new mouse line where *Bmi1* can be conditionally overexpressed in a hematopoietic cell-specific fashion and analyzed the effect of overexpression of *Bmi1* in detail. Overexpression of *Bmi1* did not significantly affect steady state hematopoiesis, but it efficiently protected HSCs from stresses. Our findings suggest that overexpression of *Bmi1* confers resistance to stresses on HSCs, thereby augmenting their regenerative capacity.

Recent findings have established that the regulation of oxidative stress in HSCs is critical for the maintenance of HSCs. In this study, we demonstrated that overexpression of *Bmi1* protects HSCs from loss of self-renewal capacity at least in part by increasing the capacity of HSCs to resist oxidative stress. It has been reported that *Bmi1*-deficient mice have an increased level of intracellular ROS due to de-regulated expression of genes related to mitochondrial function and ROS generation [24,25]. However, an excess of Bmi1 in this study had no effect on the levels of intracellular ROS. Thus, it is hypothesized that Bmi1 is negatively regulated downstream of the ROS signal and an excess of Bmi1 overcomes this negative regulation. Indeed, ROS reportedly primes *Drosophila* hematopoietic progenitors for differentiation and this process involves downregulation of PcG activity [26]. ROS signaling activates p38 and eventually releases the transcriptional repression of *p16^{Ink4a}* and *p19^{Arf}*, critical targets of Bmi1 [16]. Furthermore, recent studies including ours have revealed that PcG proteins are downregulated and dissociate from the *Ink4a/Arf* locus when cells are exposed to intra- or extracellular stress, including tissue culture- and oncogene-induced stress

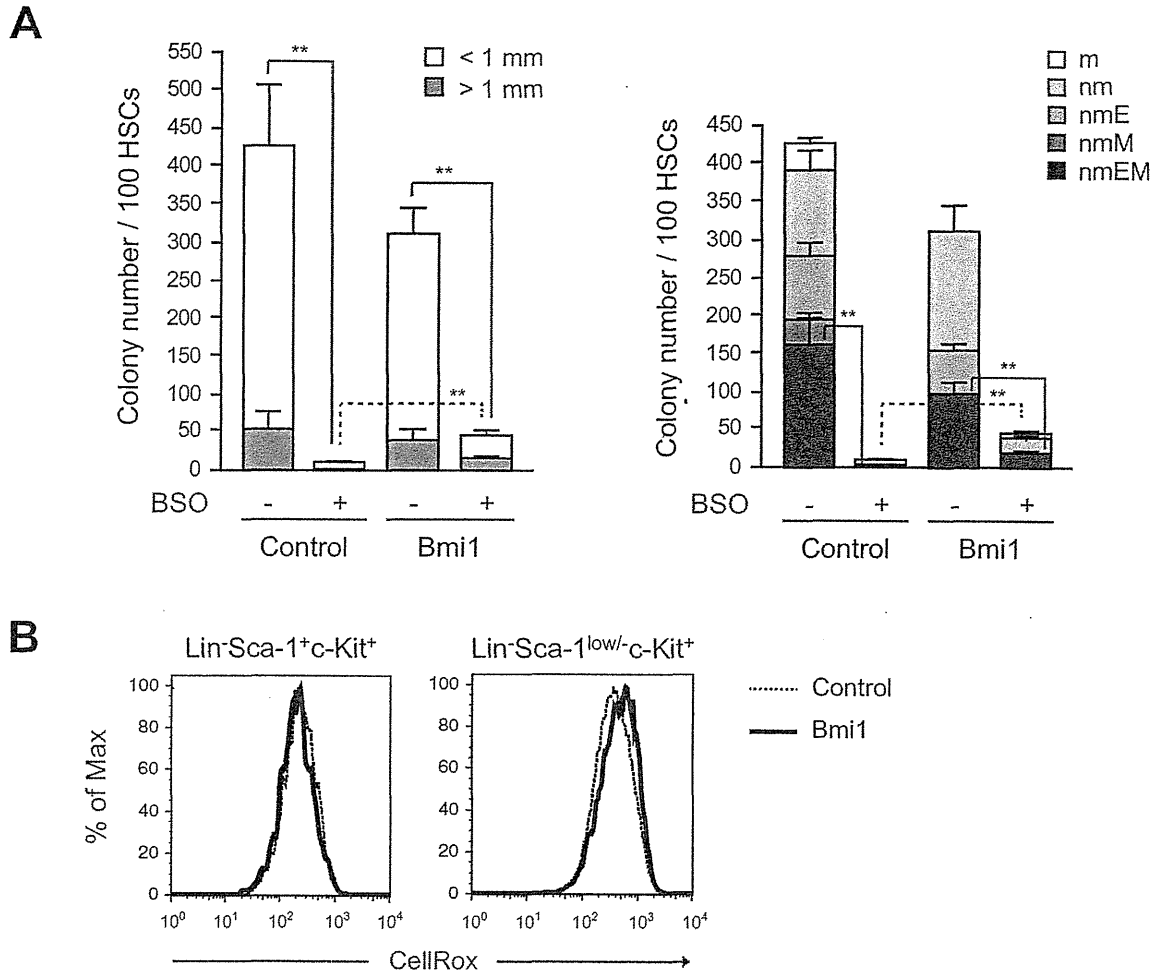
A
Colony number / 100 HSCs
< 1 mm
> 1 mm
m
nm
nmE
nmM
nmEM
BSO
Control
Bmi1
B
Lin-Sca-1+c-Kit+
Lin-Sca-1low/-c-Kit+
% of Max
Control
Bmi1
CellRox
C
Tie2-Cre; NAC(-)
Tie2-Cre;R26StopFLBmi1; NAC(-)
Tie2-Cre; 150 μM NAC
Tie2-Cre;R26StopFLBmi1; 150 μM NAC
Lineage marker
c-Kit
Sca-1
6.82
0.19
24.0
1.24
8.72
0.50
17.6
2.39

Figure 6. Overexpression of Bmi1 confers oxidative stress on HSCs. (A) Colony formation by HSCs cultured for 3 days. $CD34^-LSK$ cells from *Tie2-Cre* (Control) and *Tie2-Cre;R26Stop^{FL}Bmi1* (Bmi1) mice were cultured in the SF-O3 serum-free medium supplemented with 50 ng/ml SCF, TPO and 0.05 mM of BSO. At day 3 of culture, the cells were plated in methylcellulose medium to allow formation of colonies in the presence of 20 ng/ml SCF, 20 ng/ml TPO, 20 ng/ml IL-3, and 3 u/ml EPO. Absolute numbers of LPP and HPP-CFCs (left panel) are shown as the mean ± S.D. for triplicate cultures. Absolute numbers of each colony types are shown in the right panel. Data are shown as the mean ± S.D. for triplicate analyses. Statistical analyses were performed on the total colony numbers (left panel) and nmEM colony numbers (right panel), respectively. $^{**}p<0.01$. (B) Levels of ROS in cells overexpressing *Bmi1*. $CD34^-LSK$ cells from *Tie2-Cre* (Control) and *Tie2-Cre;R26Stop^{FL}Bmi1* (Bmi1) mice were cultured in the SF-O3 serum-free medium supplemented with 50 ng/ml SCF and TPO. Representative flow cytometric profiles of LSK and Lineage marker$^-$Sca-$1^{low/-}$c-Kit^+ cells in cultures at day 14 are depicted. (C) Effects of NAC on *Bmi1* culture. $CD34^-LSK$ cells from *Tie2-Cre* and *Tie2-Cre;R26Stop^{FL}Bmi1* mice were cultured in the SF-O3 serum-free medium supplemented with 50 ng/ml SCF and TPO in the presence and absence of 150 μM NAC. Representative flow cytometric profiles of LSK cells in cultures at day 14 are depicted. The proportion of Lin^- and LSK cells in total cells are indicated.
doi:10.1371/journal.pone.0036209.g006

[27,28]. Together, this accumulating evidence suggests that Bmi1 is dynamically regulated in response to oxidative stress, probably downstream of p38. Our preliminary data demonstrated that activated p38 directly phosphorylates Bmi1 *in vitro* (Oshima and Iwama., unpublished data). Thus, it is possible that p38, which is activated by oxidative stress, attenuates Bmi1 function via direct phosphorylation of Bmi1. How oxidative stress restricts the expression and function of Bmi1 is an important issue to be addressed.

Of note, the effect of Bmi1 overexpression in serial transplantation resembles that of overexpression of *Ezh2*, a gene encoding a core component of PRC2 [29]. Overexpression of PcG genes, *Bmi1* and *Scmh1*, also induces tolerance of cortical neurons to ischemia [30]. Thus, various cellular stresses may target PcG complexes to release transcriptional repression of PcG-regulated genes, such as tumor suppressor and developmental regulator genes, thereby affecting stemness. All these findings support the notion that enforcement of PcG function is a key for successful regenerative therapies.

Meanwhile, the role of PcG proteins in resistance to oxidative stress is also implicated in cancer. Expression of PcG proteins including *BMI1* and *EZH2* are often up-regulated in various cancers, particularly in their cancer stem cell fractions [31]. Interestingly, cancer stem cells in some tumors appear to be susceptible to ROS, similar to normal stem cells, and thus develop mechanisms to keep the levels of ROS low [32]. Interference of EZH2 function by the small-molecule histone methyltransferases inhibitor, DZNep, is reported to increase ROS levels in acute myeloid leukemia cells like in *Bmi1*-deficient mice [33]. Conversely, our findings in this study suggest that an excess of PcG proteins often observed in aggressive cancer could help cancer stem cells tolerate oxidative stress. In this regard, overexpression of PcG proteins could also be therapeutic targets in cancers including leukemia. Finally, no *Tie2-Cre;R26Stop^{FL}Bmi1* mice developed hematological malignancies during the observation period, up to 18 months after birth. Only one recipient mice with *Tie2-Cre;R26Stop^{FL}Bmi1* BM cells developed acute lymphocytic leukemia in the tertiary transplantation. These findings suggest that Bmi1 by itself is not sufficient to induce hematological malignancies.

Methods

Ethics Statement

All experiments using the mice were performed in accordance with our institutional guidelines for the use of laboratory animals and approved by the review board for animal experiments of Chiba University (approval ID: 21–150).

Generation of Mice

To generate tissue-specific *Bmi1*-transgenic mice, we used the plasmid *R26Stop^{FL}*, a modified version of pROSA26-1 with a *loxP*-flanked *neo^r*-stop cassette, an *frt*-flanked *IRES-eGFP* cassette, and a bovine polyadenylation sequence [34]. We cloned a cDNA encoding a flag-tagged *Bmi1* upstream of the *IRES* sequence (*R26Stop^{FL}Bmi1*). R1 ES cells were transfected, cultured, and selected as previously described [35]. For conditional expression of *Bmi1*, the *RosaStop^{FL}Bmi1* mice were crossed with *Tie2-Cre* mice. C57BL/6 (CD45.2) mice were purchased from Japan SLC (Shizuoka, Japan). C57BL/6 mice congenic for the Ly5 locus (CD45.1) were purchased from Sankyo-Lab Service (Tsukuba, Japan). Mice were bred and maintained in the Animal Research Facility of the Graduate School of Medicine, Chiba University in accordance with institutional guidelines. This study was approved by the institutional review committees of Chiba University (approval numbers 21–65 and 21–150).

Flow Cytometric Analysis and Cell Sorting

Mouse $CD34^-LSK$ HSCs were purified from BM of 8–12-week-old mice. Mononuclear cells were isolated on Ficoll-Paque PLUS (GE Healthcare). Cells were stained with an antibody cocktail consisting of biotinylated anti-Gr-1, Mac-1, interleukin (IL)-7Rα, B220, CD4, CD8α, and Ter119 monoclonal antibodies. The monoclonal antibodies were purchased from eBioScience or BioLegend. Lineage-positive cells were depleted with goat anti-rat IgG microbeads (Miltenyi Biotec) through an LS column (Miltenyi Biotec). Cells were further stained with Alexa Fluor® 647 or eFluor® 660-conjugated anti-CD34, phycoerythrin (PE)-conjugated anti-Sca-1, and phycoerythrin/Cy7 (PE/Cy7)-conjugated anti-c-Kit antibodies. Biotinylated antibodies were detected with allophycocyanin/Cy7 (APC/Cy7)-conjugated streptavidin. Dead cells were eliminated by staining with Propidium iodide (1 μg/ml, Sigma). Analysis and sorting were performed on a FACS Aria II (BD Bioscience).

Cell Cycle Analysis

Fresh BM cells (1×10^7, CD45.2) were transplanted into 8-week-old CD45.1 mice irradiated at a dose of 9.5 Gy without competitor cells. Four months later, BM mononuclear cells were isolated on Ficoll-Paque PLUS. Cells were stained with an antibody cocktail consisting of biotinylated anti-Gr-1, Mac-1, IL-7Rα, B220, CD4, CD8α, Ter119, and CD45.1 monoclonal antibodies. Cells were further stained with Alexa Fluor® 700-conjugated anti-CD34, pacific blue-conjugated anti-Sca-1, and APC-conjugated anti-c-Kit antibodies. Biotinylated antibodies were detected with APC/Cy7-conjugated streptavidin. Analysis was performed on a FACS Aria II. To analyze the cell-cycle status, cells were incubated with 1 μg/ml Pyronin Y (Sigma) at 37°C for 45 min with protection from light. Bulk sorted $CD34^-LSK$ cells were incubated in SF-O3 supplemented with 50 μM?2-β-mercaptoethanol, 0.2% BSA, 1% GPS, 50 ng/ml SCF, 50 ng/ml TPO for 10 days at 37°C in a 5% CO_2 atmosphere. At day 10 of culture, the cell cycle profiles of culture cells were analyzed using an APC BrdU Flow Kit (BD Pharmingen). The cells were incubated with 10 μM BrdU at 37°C for 30 min and then stained with an antibody cocktail consisting of biotinylated anti-Gr-1,

Mac-1, IL-7Rα, B220, CD4, CD8α, and Ter119 monoclonal antibodies. Cells were further stained with PE-conjugated anti-Sca-1, and PE/Cy7-conjugated anti-c-Kit antibodies. Biotinylated antibodies were detected with APC/Cy7-conjugated streptavidin. Analysis was performed on a FACS Canto II (BD Bioscience).

Colony Assay

Colony assays were performed in methylcellulose-containing Iscove's modified Dulbecco's medium (Methocult M3234; Stemcell Technologies) supplemented with 20 ng/ml mouse SCF, 20 ng/ml mouse IL-3, 20 ng/ml human TPO, and 3 U/ml human EPO (Peprotech), and incubated at 37°C in a 5% CO_2 atmosphere. The number of HPP- and LPP-colony-forming cells (CFCs), which generate a colony with a diameter ≥1 mm and <1 mm, respectively, were evaluated by counting colonies at day 10–14 of culture. Colonies were individually collected, cytospun onto glass slides, and subjected to Hemacolor (MERCK) staining for morphological examination. To evaluate the proliferative and differentiation capacity of *Tie2-Cre;R26Stop^{FL}Bmi1* HSCs *in vitro*, single CD34$^-$LSK HSCs were clonally sorted into 96-microtiter plates containing 100 µl SF-O3 (Sanko Junyaku) supplemented with 50 µM 2-β-mercaptoethanol, 10% FBS, 1% L-glutamine, penicillin, streptomycin solution (GPS; Sigma), 10 ng/ml mouse SCF, 10 ng/ml human TPO, 10 ng/ml mouse IL-3, and 3 unit/ml human EPO (PeproTech). At day 14 of culture, the colonies were counted and individually collected for morphological examination. To evaluate the tolerance of test cells against oxidative stress, CD34$^-$LSK cells were cultured in the presence of DL-Buthionin-(*S,R*)-sulfoximine (BSO, Sigma) or *N*-Acetyl-L-cysteine (NAC, Sigma) for the indicated time periods, then subjected to colony assays or flow cytometric analyses.

Serial Transplantation and CRU Assays

Fresh BM cells (5×10^5, CD45.2) or 10-day cultured CD34$^-$LSK cells (CD45.2) corresponding to 20 initial CD34$^-$LSK cells were transplanted into 8-week-old recipient mice (CD45.1) irradiated at a dose of 9.5 Gy together with 5×10^5 and 2×10^5 BM competitor cells from 8-week-old CD45.1 mice, respectively. For serial transplantation, BM cells were collected from all recipient mice at 12–20 weeks after transplantation and pooled together. Then, 5×10^6 BM cells were transplanted into 8-week-old B6-CD45.1 mice irradiated at a dose of 9.5 Gy without competitor cells. Third and fourth transplantation were similarly performed using 5×10^6 pooled BM cells. Peripheral blood (PB) cells of the recipient mice were analyzed with a mixture of antibodies that included PE/Cy7-conjugated anti-CD45.1, pacific blue-conjugated anti-CD45.2, PE-conjugated anti-Mac-1 and anti-Gr-1, APC-conjugated anti-B220, and APC/Cy7-conjugated anti-CD4 and anti-CD8α antibodies. Cells were analyzed on a FACS Canto II. Percent donor chimerism was calculated as (% donor cells) ×100/(% donor cells + % recipient cells). To obtain the competitive repopulating units (CRUs), CRU assays were performed with a limiting number of test cells and the data were analyzed using L-Calc software (StemCell Technologies). Peripheral blood cell counts were made using an automated cell counter, Celltec α (Nihon Kohden).

Apoptosis Analysis

Bulk sorted CD34$^-$LSK cells were incubated in SF-O3 supplemented with 50 µM?2-β-mercaptoethanol, 0.2% BSA, 1% GPS, 50 ng/ml SCF, 50 ng/ml TPO for 10 days at 37°C in a 5% CO_2 atmosphere. At day 10 of culture, the cultured cells were incubated with APC-conjugated anti-Annexin V (BD Pharmingen) and propidium iodide at room temperature for 15 min with protection from light. Analysis was performed on FACS Canto II.

Immunostaining of γH2A.X

Cells were incubated in a culture medium drop on slide glasses pre-treated with poly-L-lysine (Sigma) for 2 hours. After fixation with 2% paraformaldehyde and blocking in 4% sheep serum for 30 min at room temperature, cells were incubated with purified anti-phospho-Histone H2A.X (Ser139) antibody (Cell Signaling Technology) for 12 hours at 4°C. The cells were then washed and incubated with Alexa Flour 555-conjugated anti-rabbit IgG goat polyclonal antibody (Invitrogen) for 60 min at room temperature. DNA was counterstained with 4′,6-diamidino-2-phenylindole (DAPI). Images were taken with a Keyence BZ-9000 fluorescence microscope.

RT-PCR

Total RNA was isolated using TRIZOL LS solution or TRIZOL solution (Invitrogen) and reverse transcribed by the ThermoScript RT-PCR system (Invitrogen) with an oligo-dT primer. Real-time quantitative polymerase chain reaction (PCR) was performed with an ABI prism 7300 Thermal Cycler (Applied Biosystems) using FastStart Universal Probe Master (Roche). The combination of primer sequences and probe numbers are as follows: for *p16^{Ink4a}*, probe #91, 5′-AATCTCCGCGAGGAAGC-3′, and 5′-GTCTGTCTGCAGCGGACTC-3′; for *p19^{Arf}*, probe #106, 5′-GGGTTTTCTTGGTGAAGTTCG-3′, 5′- TTGCCCATCATCATCACCT-3′, and for *Bmi1*, probe #95, 5′-AAACCAGACCACTCCTGAACA-3′ and 5′-TCTTCTTCTCTTCATCTCATTTTTGA-3′.

Western Blotting

Total cell lysate was resolved by SDS-PAGE and transferred to a PVDF membrane. The blots were probed with a mouse anti-Bmi1 (clone 8A9, kindly provided by Dr. N. Nozaki, MAB Institute, Co. Ltd., Japan), and a horseradish peroxidase-conjugated secondary antibody. The protein bands were detected with an enhanced chemiluminescence reagent (SuperSignal, Pierce Biotechnology).

Detection of ROS

Cells were stained with an antibody cocktail consisting of biotinylated anti-Gr-1, Mac-1, IL-7Rα, B220, CD4, CD8α, and Ter119 monoclonal antibodies. Cells were further stained with PE-conjugated anti-Sca-1, and PE/Cy7-conjugated anti-c-Kit antibodies. Biotinylated antibodies were detected with APC/Cy7-conjugated streptavidin. After staining with antibodies, cells were incubated with CellROX^{TM} Deep Red Reagent (5 µM, Invitrogen) at 37°C for 30 min with protection from light. Dead cells were eliminated by staining with propidium iodide (1 µg/ml, Sigma). Analysis was performed on a FACS Aria II.

Supporting Information

Figure S1 Steady state hematopoiesis in *Tie2-Cre;R26-StopFLBmi1* mice. (A) Hematopoietic analysis of 10-week-old *Tie2-Cre* and *Tie2-Cre;R26Stop^{FL}Bmi1* mice. Absolute numbers of CMPs, GMPs, MEPs, and CLPs in bilateral femurs and tibiae (upper panels), total spleen cells and LSK cells in the spleen (middle panel), and total thymic cells, CD4+CD8- cells, CD4-CD8+ cells, and CD4+CD8+ cells in the thymus (lower panels) are shown as the mean ± S.D. (*Tie2-Cre*; n = 8, *Tie2-Cre;R26-Stop^{FL}Bmi1*; n = 7). (B) Cell cycle status of CD34-LSK cells examined by Pyronin Y incorporation. Proportion of CD34-

LSK cells in the G0 phase of the cell cycle (Pyronin Y-) was shown as the mean ± S.D. (n = 4) (left panel). Representative flow cytometric profiles are also depicted (right panel).
(EPS)

Figure S2 Apoptosis and cell cycle status of *Tie2-Cre;R26Stop^{FL}Bmi1* LSK cells in culture. (A) The proportion of apoptotic cells in the LSK fraction in culture. CD34-LSK cells from *Tie2-Cre* (Control) and *Tie2-Cre;R26Stop^{FL}Bmi1* (Bmi1) mice were cultured in the SF-O3 serum-free medium supplemented with 50 ng/ml SCF and TPO. At day 10 of culture, apoptotic cells were detected by staining culture cells with anti-Annexin V and propidium iodide (PI). The percentage of Annexin V+PI- apoptotic cells in the LSK fraction is shown as the mean ± S.D. (n = 5). (B) The cell cycle status of LSK cells overexpressing Bmi1. CD34-LSK cells from *Tie2-Cre* (Control) and *Tie2-Cre;R26-Stop^{FL}Bmi1* (Bmi1) mice were cultured in the SF-O3 serum-free medium supplemented with 50 ng/ml SCF and TPO. At day 10 of culture, the cells were incubated with 10 μM BrdU at 37°C for 30 min and then analyzed using a BrdU Flow Kit. Data are shown as the mean ± SD (n = 4).
(EPS)

Figure S3 Hematopoietic recovery in recipients of *Tie2-Cre;R26Stop^{FL}Bmi1* HSCs after irradiation. Fresh BM cells from *Tie2-Cre* and *Tie2-Cre;R26Stop^{FL}Bmi1* mice (1×107, CD45.2) were transplanted into 8-week-old CD45.1 mice irradiated at a dose of 9.5 Gy without competitor cells. Four months later, the recipient mice were irradiated at a dose of 5 Gy. Changes in the PB cell count were monitored for 4 weeks (A) and the absolute number of BM LSK cells in bilateral femurs and tibiae was examined at 4 weeks post-irradiation (B). Data are shown as the mean ± SD (n = 5).
(EPS)

Figure S4 ROS levels in *Tie2-Cre;R26Stop^{FL}Bmi1* cells in culture. Levels of ROS in cells overexpressing Bmi1 in culture. CD34-LSK cells from *Tie2-Cre* (Control) and *Tie2-Cre;R26-Stop^{FL}Bmi1* (Bmi1) mice were cultured in the SF-O3 serum-free medium supplemented with 50 ng/ml SCF and TPO. Cells from day 11 or 12 of culture were further cultured for 2 days in the presence of 0.2 mM BSO, then levels of ROS in Lin-Sca-1+c-Kit+ cells and Lin-Sca-1low/−c-Kit+ cells were analyzed using CellROXTM Deep Red Reagent. Data are shown as dots and the mean values are indicated by bars (n = 4).
(EPS)

Acknowledgments

We thank Naohito Nozaki for the anti-Bmi1 antibody, George Wendt for critical reading of the manuscript, and Mieko Tanemura for laboratory assistance.

Author Contributions

Conceived and designed the experiments: SN AI. Performed the experiments: SN M. Oshima JY AS SM TK SY M. Osawa. Analyzed the data: SN AI. Contributed reagents/materials/analysis tools: HK HN. Wrote the paper: SN AI.

References

1. Simon JA, Kingston RE (2009) Mechanisms of polycomb gene silencing: knowns and unknowns. Nat Rev Mol Cell Biol 10: 697–708.
2. Iwama A, Oguro H, Negishi M, Kato Y, Nakauchi H (2005) Epigenetic regulation of hematopoietic stem cell self-renewal by polycomb group genes. Int J Hematol 81: 294–300.
3. Konuma T, Oguro H, Iwama A (2010) Role of the polycomb group proteins in hematopoietic stem cells. Dev Growth Differ 52: 505–516.
4. Sauvageau M, Sauvageau G (2010) Polycomb group proteins: multi-faceted regulators of somatic stem cells and cancer. Cell Stem Cell 7: 299–313.
5. Lessard J, Sauvageau G (2003) Bmi-1 determines the proliferative capacity of normal and leukaemic stem cells. Nature 423: 255–260.
6. Park IK, Qian D, Kiel M, Becker MW, Pihalja M, et al. (2003) Bmi-1 is required for maintenance of adult self-renewing haematopoietic stem cells. Nature 423: 302–305.
7. Iwama A, Oguro H, Negishi M, Kato Y, Morita Y, et al. (2004) Enhanced self-renewal of hematopoietic stem cells mediated by the polycomb gene product Bmi-1. Immunity 21: 843–851.
8. Oguro H, Iwama A, Morita Y, Kamijo T, van Lohuizen M, et al. (2006) Differential impact of Ink4a and Arf on hematopoietic stem cells and their bone marrow microenvironment in Bmi1-deficient mice. J Exp Med 203: 2247–2253.
9. Oguro H, Yuan J, Ichikawa H, Ikawa T, Yamazaki S, et al. (2010) Poised lineage specification in multipotent hematopoietic stem and progenitor cells by the polycomb protein Bmi1. Cell Stem Cell 6: 279–286.
10. Mihara K, Chowdhury M, Nakaju N, Hidani S, Ihara A, et al. (2006) Bmi-1 is useful as a novel molecular marker for predicting progression of myelodysplastic syndrome and patient prognosis. Blood 107: 305–308.
11. Rizo A, Horton SJ, Olthof S, Dontje B, Ausema A, et al. (2010) BMI1 collaborates with BCR-ABL in leukemic transformation of human CD34+ cells. Blood 116: 4621–4630.
12. Kisanuki YY, Hammer RE, Miyazaki J, Williams SC, Richardson JA, et al. (2001) Tie2-Cre transgenic mice: a new model for endothelial cell-lineage analysis in vivo. Dev Biol 230: 230–242.
13. Takano H, Ema H, Sudo K, Nakauchi H (2004) Asymmetric division and lineage commitment at the level of hematopoietic stem cells: inference from differentiation in daughter cell and granddaughter cell pairs. J Exp Med 199: 295–302.
14. Ema H, Takano H, Sudo K, Nakauchi H (2000) In vitro self-renewal division of hematopoietic stem cells. J Exp Med 192: 1281–1288.
15. Shima H, Takubo K, Iwasaki H, Yoshihara H, Gomei Y, et al. (2009) Reconstitution activity of hypoxic cultured human cord blood CD34-positive cells in NOG mice. Biochem Biophys Res Commun 378: 467–472.
16. Ito K, Hirao A, Arai F, Takubo K, Matsuoka S, et al. (2006) Reactive oxygen species act through p38 MAPK to limit the lifespan of hematopoietic stem cells. Nat Med 12: 446–451.
17. Yahata T, Takanashi T, Muguruma Y, Ibrahim AA, Matsuzawa H, et al. (2011) Accumulation of oxidative DNA damage restricts the self-renewal capacity of human hematopoietic stem cells. Blood 118: 2941–2950.
18. Rossi DJ, Jamieson CH, Weissman IL (2008) Stems cells and the pathways to aging and cancer. Cell 132: 681–696.
19. Chagraoui J, Hébert J, Girard S, Sauvageau G (2011) An anticlastogenic function for the Polycomb Group gene Bmi1. Proc Natl Acad Sci USA 108: 5284–5289.
20. Ginjala V, Nacerddine K, Kulkarni A, Oza J, Hill SJ, et al. (2011) BMI1 is recruited to DNA breaks and contributes to DNA damage-induced H2A ubiquitination and repair. Mol Cell Biol 31: 1972–1982.
21. Facchino S, Abdouh M, Chatoo W, Bernier G (2010) BMI1 confers radioresistance to normal and cancerous neural stem cells through recruitment of the DNA damage response machinery. J Neurosci 30: 10096–10111.
22. Shao L, Li H, Pazhanisamy SK, Meng A, Wang Y, et al. (2010) Reactive oxygen species and hematopoietic stem cell senescence. Int J Hematol 94: 24–32.
23. Jang YY, Sharkis SJ (2007) A low level of reactive oxygen species selects for primitive hematopoietic stem cells that may reside in the low-oxygenic niche. Blood 110: 3056–3063.
24. Liu J, Liu C, Chen J, Song S, Lee IH, et al. (2009) Bmi1 regulates mitochondrial function and the DNA damage response pathway. Nature 459: 387–392.
25. Rizo A, Olthof S, Han L, Vellenga E, de Haan G, et al. (2009) Repression of BMI1 in normal and leukemic human CD34$^+$ cells impairs self-renewal and induces apoptosis. Blood 114: 1498–1505.
26. Owusu-Ansah E, Banerjee U (2009) Reactive oxygen species prime Drosophila haematopoietic progenitors for differentiation. Nature 461: 537–541.
27. Bracken AP, Kleine-Kohlbrecher D, Dietrich N, Pasini D, Gargiulo G, et al. (2007) The polycomb group proteins bind throughout the INK4A-ARF locus and are disassociated in senescent cells. Genes Dev 21: 525–530.
28. Negishi M, Saraya A, Mochizuki S, Helin K, Koseki H, et al. (2010) A novel zinc finger protein Zfp277 mediates transcriptional repression of the Ink4a/Arf locus through polycomb repressive complex 1. PLoS One 5: e12373.
29. Kamminga LM, Bystrykh LV, de Boer A, Houwer S, Douma J, et al. (2006) The Polycomb group gene Ezh2 prevents hematopoietic stem cell exhaustion. Blood 107: 2170–2179.
30. Stapels M, Piper C, Yang T, Li M, Stowell C, et al. (2010) Polycomb group proteins as epigenetic mediators of neuroprotection in ischemic tolerance. Sci Signal 3: ra15.
31. Bracken AP, Helin K (2009) Polycomb group proteins: navigators of lineage pathways led astray in cancer. Nat Rev Cancer 9: 773–784.

32. Diehn M, Cho RW, Lobo NA, Kalisky T, Dorie MJ, et al. (2009) Association of reactive oxygen species levels and radioresistance in cancer stem cells. Nature 458: 780–783.
33. Zhou J, Bi C, Cheong LL, Mahara S, Liu SC, et al. (2011) The histone methyltransferase inhibitor, DZNep, up-regulates TXNIP, increases ROS production, and targets leukemia cells in AML. Blood 118: 2830–2839.
34. Sasaki Y, Derudder E, Hobeika E, Pelanda R, Reth M, et al. (2006) Canonical NF-kappaB activity, dispensable for B cell development, replaces BAFF-receptor signals and promotes B cell proliferation upon activation. Immunity 24: 729–739.
35. Fukamachi H, Fukuda K, Suzuki M, Furumoto T, Ichinose M, et al. (2001) Mesenchymal transcription factor Fkh6 is essential for the development and differentiation of parietal cells. Biochem Biophys Res Commun 280: 1069–1076.

Regular Article

HEMATOPOIESIS AND STEM CELLS

Role of SOX17 in hematopoietic development from human embryonic stem cells

Yaeko Nakajima-Takagi,[1,2] Mitsujiro Osawa,[1,2] Motohiko Oshima,[1,2] Haruna Takagi,[1] Satoru Miyagi,[1,2] Mitsuhiro Endoh,[2,3] Takaho A. Endo,[3,4] Naoya Takayama,[5,6] Koji Eto,[5,6] Tetsuro Toyoda,[4] Haruhiko Koseki,[2,3] Hiromitsu Nakauchi,[6] and Atsushi Iwama[1,2]

[1]Department of Cellular and Molecular Medicine, Graduate School of Medicine, Chiba University, Chiba, Japan; [2]JST, CREST, Tokyo, Japan; [3]RIKEN Research Center for Allergy and Immunology, Yokohama, Japan; [4]RIKEN Genomic Sciences Center, Yokohama, Japan; [5]Center for iPS Cell Research and Application, Kyoto University, Kyoto, Japan; and [6]Division of Stem Cell Therapy, Center for Stem Cell Biology and Regenerative Medicine, Institute of Medical Science, University of Tokyo, Tokyo, Japan

Key Points

- SOX17 plays a key role in priming hemogenic potential in endothelial cells during hematopoietic development from ES cells.

To search for genes that promote hematopoietic development from human embryonic stem cells (hESCs) and induced pluripotent stem cells (iPSCs), we overexpressed several known hematopoietic regulator genes in hESC/iPSC-derived CD34$^+$CD43$^-$ endothelial cells (ECs) enriched in hemogenic endothelium (HE). Among the genes tested, only *Sox17*, a gene encoding a transcription factor of the SOX family, promoted cell growth and supported expansion of CD34$^+$CD43$^+$CD45$^{-/low}$ cells expressing the HE marker VE-cadherin. *SOX17* was expressed at high levels in CD34$^+$CD43$^-$ ECs compared with low levels in CD34$^+$CD43$^+$CD45$^-$ pre-hematopoietic progenitor cells (pre-HPCs) and CD34$^+$CD43$^+$CD45$^+$ HPCs. *Sox17*-overexpressing cells formed semiadherent cell aggregates and generated few hematopoietic progenies. However, they retained hemogenic potential and gave rise to hematopoietic progenies on inactivation of Sox17. Global gene-expression analyses revealed that the CD34$^+$CD43$^+$CD45$^{-/low}$ cells expanded on overexpression of *Sox17* are HE-like cells developmentally placed between ECs and pre-HPCs. *Sox17* overexpression also reprogrammed both pre-HPCs and HPCs into HE-like cells. Genome-wide mapping of Sox17-binding sites revealed that Sox17 activates the transcription of key regulator genes for vasculogenesis, hematopoiesis, and erythrocyte differentiation directly. Depletion of *SOX17* in CD34$^+$CD43$^-$ ECs severely compromised their hemogenic activity. These findings suggest that SOX17 plays a key role in priming hemogenic potential in ECs, thereby regulating hematopoietic development from hESCs/iPSCs. (*Blood.* 2013;121(3):447-458)

Introduction

During mammalian development, 2 waves of hematopoiesis occur in sequential stages: first, a transient wave of primitive hematopoiesis, followed by definitive hematopoiesis. These stages are temporally and anatomically distinct and involve unique cellular and molecular regulators. The formation of primitive blood cells occurs early during fetal life, with coordinated progression from extraembryonic to intraembryonic sites of hematopoiesis. Within the embryo, definitive hematopoiesis undergoes developmentally stereotyped transitions: hematopoietic stem cells (HSCs) arising from the aorta-gonad-mesonephros region migrate first to the placenta and fetal liver and then to the spleen. Eventually, hematopoiesis shifts to the BM, where homeostatic blood formation is maintained postnatally.[1]

During definitive fetal hematopoiesis, HSCs emerge directly from a small population of endothelial cells (ECs) in the conceptus, referred to as the "hemogenic endothelium" (HE).[2-4] HE is located in all sites of HSC emergence, including the ventral aspect of the dorsal aorta, vitelline and umbilical arteries, yolk sac, and placenta. The process by which blood forms from HE involves an endothelial-to-hematopoietic cell transition during which individual cells bud out and detach from the endothelial layer.[2-4] HE is distinguished from all other ECs by the presence of a transcription factor called Runx1.[5] Runx1 is expressed in HE cells, in newly formed hematopoietic cell clusters, and in all functional HSCs.[6,7] A similar process occurs during hemangioblast differentiation in primitive blood cell formation. The extraembryonic yolk sac is considered to be the first site of emergence of the "hemangioblast," a mesodermal precursor with both endothelial and hematopoietic potential. Hemangioblasts differentiate into a HE intermediate, which gives rise to primitive hematopoietic cells but also definitive hematopoietic cells on activation of Runx1.[8]

Human embryonic stem cells (hESCs) and induced pluripotent stem cells (iPSCs) have been demonstrated to reproduce many aspects of embryonic hematopoiesis in stromal coculture or embryoid body (EB) culture. A recent study has provided evidence that hematopoietic differentiation of hESCs progresses through

Submitted May 19, 2012; accepted October 31, 2012. Prepublished online as *Blood* First Edition paper, November 20, 2012; DOI 10.1182/blood-2012-05-431403.

There is an Inside *Blood* commentary on this article in this issue.

The online version of this article contains a data supplement.

The publication costs of this article were defrayed in part by page charge payment. Therefore, and solely to indicate this fact, this article is hereby marked "advertisement" in accordance with 18 USC section 1734.

sequential stages: first is the HE, then primitive hematopoiesis, and finally definitive hematopoiesis, a process resembling the development of physiologic hematopoiesis.[9] However, the induction of hematopoietic cells from hESCs/iPSCs is still inefficient. Significant innovations are required before it will be possible to obtain sufficient numbers of the specific types of hematopoietic cells needed for therapeutic uses.

Sry-related high-mobility group box 17 (SOX17) is a member of the SOX family of DNA-binding transcription factors. Sox17 participates in various developmental processes and biologic activities, such as formation of definitive endoderm[10] and vascular development.[11] Moreover, recent studies have shown that Sox17 also plays an important role in fetal hematopoiesis in the yolk sac and fetal liver, especially in the maintenance of fetal and neonatal HSCs, but not adult HSCs.[12] Overexpression of *Sox17* has also been shown to confer fetal HSC characteristics onto adult hematopoietic progenitors.[13] Among SOX family members, Sox7, Sox17, and Sox18 are highly related and constitute the Sox subgroup F (SoxF). Sox7 and Sox18 are transiently expressed in hemangioblasts and hematopoietic precursors, respectively, at the onset of blood specification. Sustained expression of Sox7 and Sox18, but not Sox17, in early hematopoietic precursors from mouse ESCs and embryos enhances their proliferation while blocking their maturation.[14,15] However, the role of Sox17 in early hematopoietic development, particularly from hESCs, has not yet been clarified. In the present study, we tested the effect of overexpression of known hematopoietic regulator genes in hiPSC-derived $CD34^+CD43^-$ ECs enriched in HE to find genes that could be manipulated to efficiently produce hematopoietic cells from hESCs. We found that *Sox17* promotes the expansion of HE-like cells. We demonstrate that SOX17 functions in HE and plays a role in the development of hematopoietic cells from hESCs/iPSCs.

Methods

Cell lines

H1 hESCs (WiCell Research Institute) and TkCBV4-7 hiPSCs generated from human cord blood (CB) $CD34^+$ cells were maintained on irradiated murine embryonic fibroblasts in DMEM-F12 (Sigma-Aldrich) supplemented with 1× MEM nonessential amino acids (Gibco-Invitrogen), 1× GlutaMAX-I (Gibco-Invitrogen), 20% knockout serum replacement (Gibco-Invitrogen), 0.1mM 2-mercaptoethanol (Sigma-Aldrich), 1% penicillin/streptomycin solution (Sigma-Aldrich), and 5 ng/mL of human basic fibroblast growth factor (ReproCELL). Every 3-4 days, the cells were dissected into clumps of approximately 300-500 cells in a dissociation solution consisting of 0.25% trypsin, 20% knockout serum replacement, and 1mM $CaCl_2$ in PBS and transferred to a new feeder layer to maintain them in an undifferentiated state. The OP9 stromal cell line was kindly provided by Toru Nakano (Osaka University, Osaka, Japan). OP9 cells were maintained in α-MEM (Gibco-Invitrogen) supplemented with 2.2 g/L of sodium bicarbonate, 20% FBS, and 1% L-glutamine and penicillin/streptomycin solution (Sigma-Aldrich).

EB differentiation

H1 hESCs or TkCBV4-7 hiPSCs were dissociated into single cells with Accumax (Innovative Cell Technologies). The cells were washed with DMEM-F12 and recultured at 1×10^6 cells per 60-mm Petri dish (Falcon) in 5-mL mTeSR1 (StemCell Technologies) supplemented with 10μM LY27632 (Cayman), 2 ng/mL of human Bone Morphogenetic Protein 4 (BMP4; PeproTech), and 2 ng/mL of human activin A (PeproTech). At day 2 of culture, EBs were split from 1 60-mm Petri dish to 2 60-mm Petri dishes and cultured in EB medium consisting of IMDM (Sigma-Aldrich) containing 15% FBS, 1× GlutaMAX I, 1% penicillin/streptomycin solution, 200 μg/mL of bovine holo transferrin (Bovogen), 50 μg/mL of ascorbic acid (Sigma-Aldrich), and 450μM 1-thioglycerol (Sigma-Aldrich) supplemented with 2 ng/mL of human BMP4 and 5 ng/mL of human VEGF (PeproTech). At day 4 of culture, medium conditions were changed as described in Figure 1B. LY363947 (Cayman) was used as an inhibitor of TGFβ signaling. EBs were constantly cultured on a shaker at 70 rpm.

Flow cytometric analysis and OP9 coculture

EBs were dissociated with 0.25% trypsin-EDTA solution (Sigma-Aldrich) and filtered through a nylon screen to obtain a single-cell suspension. Flow cytometric analysis and cell sorting were performed using a FACSAria II cell sorter (BD Biosciences) and the data were analyzed using FlowJo Version 9.5.3 software (TreeStar). The following Abs were used for the flow cytometric analysis: CD34 (clone 581; Alexa Fluor 647 or PE-Cy7), CD43 (clone CD43-10G7; PE), CD45 (clone HI30; PE-Cy7), CD11b (clone M1/70; Brilliant Violet 421), CD235a (clone HIR2; PE), CD144 (VE-Cad; clone 16B1; PE), and CD309 (KDR; clone HKDR-1; APC). Sorted cells were resuspended in hematopoietic medium (IMDM, 10% FBS, 1% L-glutamine and penicillin/streptomycin solution) supplemented with 20 ng/mL of human SCF and 20 ng/mL of human thrombopoietin (TPO; PeproTech), and transferred onto semiconfluent irradiated OP9 cells. For mature hematopoietic cell differentiation, sorted cells were resuspended in HE medium supplemented with 20 ng/mL of SCF, 20 ng/mL of TPO, 10 ng/mL of human IL-3 (PeproTech), and 3 units/mL of human erythropoietin.

Retrovirus and lentivirus vectors, virus production, and transduction

Mouse *Sox17* fused to *ERT* with a 1× or 3× Flag tag was subcloned into the MIG retrovirus vector, which contains the long-terminal repeats from the murine stem cell virus and an internal ribosomal entry site upstream of the enhanced green fluorescent protein (GFP) as a marker gene. A recombinant vesicular stomatitis virus glycoprotein–pseudotyped high-titer retrovirus was generated using a 293gpg packaging cell line.[16] The virus containing media from the 293gpg cell cultures was concentrated by centrifugation at 6000*g* for 16 hours. To knock down *SOX17*, lentiviral vectors (CS-H1-shRNA-EF-1α-EGFP) expressing shRNA against human *SOX17* and *luciferase* were prepared. Target sequences were as follows; Sh-*SOX17*#1143: GCATGACTCCGGTGTGAAT, and Sh-*SOX17*#1273; GGCCAGAAGCAGTGTTACA. The viruses were produced as described previously.[17] EBs at approximately day 5-12 of culture were dissociated and the indicated cell populations were sorted using a FACSAria II. Sorted cells were seeded onto semiconfluent irradiated OP9 cells and transduced with a *SOX17-ERT* retrovirus or a *SOX17* knock-down virus. Transduced cells were cocultured with OP9 cells in the presence of the indicated cytokines. To induce nuclear translocation of SOX17-ERT, 4-hydroxy tamoxifen (4-OHT) was added to the medium to a concentration of 200nM on the following day.

Quantitative RT-PCR analysis

Total RNA was extracted using TRIzol reagent according to the manufacturer's instructions (Invitrogen). cDNA was synthesized from total RNA using ThermoScript RT-PCR System (Invitrogen). Quantitative RT-PCR was carried out using FastStart Universal Probe Master (Roche Applied Science), the Universal Probe Library (Roche Applied Science), and the Applied Biosystems 7300 Fast Real-Time PCR system (Applied Biosystems). Primer sequences and probe numbers used are listed in supplemental Methods (available on the *Blood* Web site; see the Supplemental Materials link at the top of the online article).

Colony-forming assay

Colony assays were performed in methylcellulose (StemCell Technologies) containing IMDM supplemented with 20 ng/mL of human SCF, 10 ng/mL of human IL-3, 10 ng/mL of human TPO, and 3 units/mL of human erythropoietin, and incubated at 37°C in a 5% CO_2 atmosphere. The colonies were counted at day 12 of culture. Images were captured by BIOREVO BZ-9000 (KEYENCE) with CFI Plan Fluor ELWD DM 20×C (Nikon) and processed using Adobe Photoshop Elements 4.0.

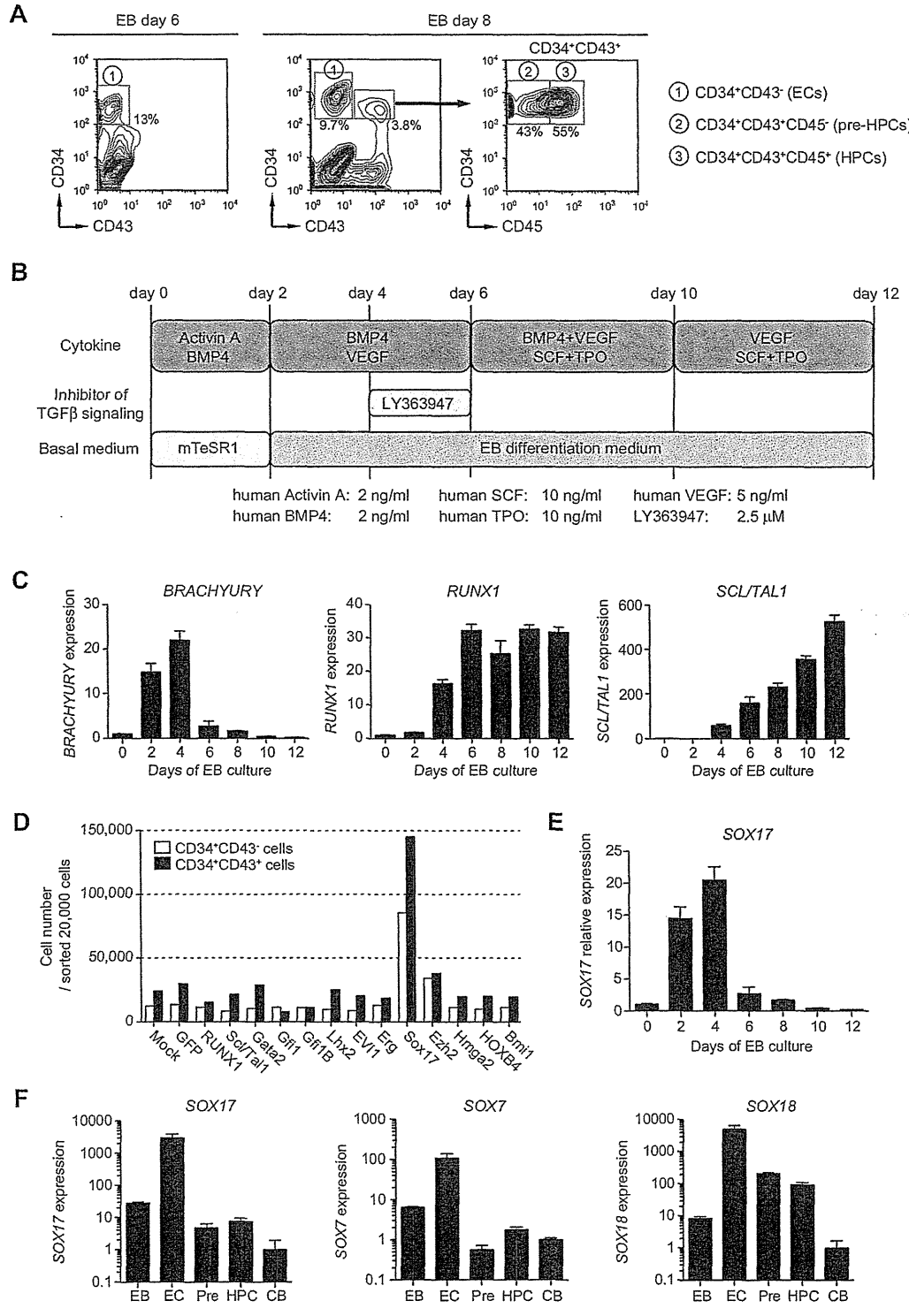

Figure 1. Screening of genes that promote expansion of hematopoietic cells from hESCs/hiPSCs. (A) Hematopoietic fractions derived from hESCs in EB culture used in this study. (B) Schematic representation of the protocol modified for efficient induction of pre-HPCs/HPCs from hESCs/hiPSCs in EB culture. (C) Expression of *BRACHYURY*, *RUNX1*, and *TAL1/SCL* expression during differentiation of hESCs in EBs determined by quantitative RT-PCR analysis. mRNA levels were normalized to *GAPDH* expression. Expression levels relative to that in hESCs (day 0 of EB culture) are shown as the means ± SD for triplicate analyses. (D) Cell growth of $CD34^+CD43^-$ cells from day 6 EBs and $CD34^+CD43^+$ cells from day 8 EBs. EBs were formed by suspension culture of hiPSCs. Sorted cells (2×10^4) were transduced with the indicated hematopoietic regulator genes and cultured on OP9 cells in the presence of 20 ng/mL of SCF and TPO. At day 14 of culture, the absolute numbers of cells were determined and are indicated in bars. Representative data from repeated experiments are shown. (E) Expression of *SOX17* during differentiation of hESCs in EBs determined by quantitative RT-PCR analysis. mRNA levels were normalized to *GAPDH* expression. Expression levels relative to that in hESCs (day 0 of EB culture) are shown as the means ± SD for triplicate analyses. (F) Expression of *SOX17*, *SOX7*, and *SOX18* in bulk EB cells, $CD34^+CD43^-$ cells (ECs), $CD34^+CD43^+CD45^-$ cells (pre-HPCs), and $CD34^+CD43^+CD45^+$ cells (HPCs) from day 8 EBs determined by quantitative RT-PCR analysis. mRNA levels were normalized to *GAPDH* expression. Expression levels relative to those in CB $CD34^+$ cells are shown as the means ± SD for triplicate analyses.

Gene-expression microarray

Total RNA was extracted using TRIzol reagent according to the manufacturer's instructions (Invitrogen). Purified total RNA was amplified and labeled using the WT expression kit (Ambion) according to the manufacturer's instructions. The labeled samples were hybridized to Human Promoter Gene 1.0 ST GeneChip arrays (Affymetrix) to assess and compare overall gene-expression profiles as described previously.[18] Microarray data were submitted to the Gene Expression Omnibus under accession number GSE38156. Expression profiles of the cells were clustered using hierarchical clustering. Distance between 2 samples was defined with the Pearson correlation using all or selected probes. Probes were selected using the Gene Ontology (GO) database or ChIP-on-chip data of Sox17.

ChIP-on-chip experiment

$CD34^+CD43^-$ cells from EBs at day 6 of culture were seeded on irradiated OP9 cells and transduced with a 3× Flag *SOX17-ERT* retrovirus. The cells were further cultured on OP9 cells in the presence of SCF, TPO (20 ng/mL), and 200nM 4-OHT. $CD34^+$ cells were collected at day 27 of culture by magnetic cell sorting using magnetic beads conjugated with anti-CD34 Abs (Miltenyi Biotec) and subjected to a ChIP assay using an anti-FLAG Ab (M2, Sigma). ChIP was carried out as described previously.[18] ChIP on chip analysis was carried out using the SurePrint G3 Human Promoter Kit, 1 × 1M (G4873A, Agilent Technologies). Purified immunoprecipitated and input DNA was subjected to T7 RNA polymerase-based amplification as described previously.[19] Labeling, hybridization, and washing were carried out according to the Agilent mammalian ChIP-on-chip protocol (Version 9.0). Scanned images were quantified with Agilent Feature Extraction software under standard conditions. The assignment of regions bound by SOX17 around transcription start sites (TSSs) was carried out using direct sequence alignment on the human genome database (National Center for Biotechnology Information Version 36). The location of SOX17-bound regions was compared with a set of transcripts derived from the MGI database. Bound regions that were within −8.0 kb to +4.0 kb of the TSS were assigned. Alignments on the human genome and TSSs of genes were retrieved from Ensembl (http://www.ensembl.org). Intensity ratios (IP/input: fold enrichment) were calculated, and the maximum value for each promoter region of a gene was used to represent the fold enrichment of the gene. Fold enrichment was calculated only for probes for which signals both from IP and input DNA were significant ($P < 10^{-3}$). ChIP-on-chip data were submitted to Gene Expression Omnibus under accession number GSE38156.

GO analysis

GO annotation was obtained using gene2go database (ftp://ftp.ncbi.nih.gov/gene/DATA/gene2go.gz) from Entrez (retrieved January 2012). Human genes were collected from the database and enrichment of SOX17-binding genes was distributed to 2 × 2 contingency tables for all GO terms (having/not having GO and binding/not binding to SOX17). We calculated P for each contingency table using hypergeometric distribution. The P value reflects the likelihood that we would observe the distribution by chance and significant GO terms were selected when $P < .001$.

Immunostaining

Sox17-ERT–transduced cells were sorted by flow cytometry and cultured on MAS-coated glass slides (Matsunami Glass Industries,) for 4 hours. The cells were then fixed with 2% paraformaldehyde and immunostained with an anti-laminin Ab (ab11575; Abcam) or an anti-FLAG Ab (M2; Sigma-Aldrich) for primary antibody reaction, and an Alexa Fluor 555 goat anti–rabbit IgG (Molecular Probes) or Alexa Fluor 555 goat anti–mouse IgG (Molecular Probes) for secondary antibody reaction, respectively. Images were captured by BIOREVO BZ-9000 (KEYENCE) with CFI Plan ApoVC 100×H (Nikon) and processed using Adobe Photoshop Elements 4.0.

Western blotting

Total cell lysate was resolved by SDS-PAGE and transferred to a PVDF membrane. The blots were probed with an anti-Sox17 Ab (09-038; Millipore) or an anti–α-tubulin (CP06; Calbiochem) and an HRP-conjugated secondary Ab. The protein bands were detected with Super-Signal West Pico Chemiluminescent Substrate (Thermo Scientific).

Results

Screening of genes that promote hematopoietic development from hESCs/iPSCs

Hematopoietic development from hESCs and hiPSCs recapitulates physiologic development, beginning in the conceptus and proceeding in a stepwise manner. $CD34^+CD43^-$ endothelial cells (ECs) enriched in HE give rise to the earliest hematopoietic progenitors, pre-hematopoietic progenitor cells (pre-HPCs) with an immunophenotype of $CD34^+CD43^+CD45^-$. Pre-HPCs then mature into $CD34^+CD43^+CD45^+$ HPCs that express CD45, a marker antigen specific to hematopoietic cells (Figure 1A).[20,21] We improved the conventional culture system to efficiently induce HPCs in EB culture by modifying cytokine conditions and adding an inhibitor of TGF-β signaling (Figure 1B). In our culture system, the expression of hematopoietic regulator genes such as *RUNX1* and *SCL/TAL1* increased in EBs after day 4 of culture accompanied by the decrease in expression of early mesodermal marker genes such as *Brachyury* (Figure 1C).

To identify genes that promote hematopoietic development from PSCs, we transduced hiPSC-derived ECs purified from day 6 EBs with several known hematopoietic regulator genes. We selected 13 genes that are known to play an important role in the development and/or maintenance of HSCs, including *RUNX1*, *Scl/Tal1*, *Gata2*, and *HOXB4*. The growth of the transduced cells was monitored in the presence of SCF and TPO for 14 days. Unexpectedly, most of these known regulator genes did not promote cell growth, but *Sox17* did. A similar effect was observed when we transduced $CD34^+CD43^+$ pre-HPCs/HPCs from day 8 EBs (Figure 1D). To confirm these findings, we overexpressed *Sox17* in hESC-derived ECs and pre-HPCs/HPCs. Overexpression of *Sox17* also promoted cell growth of hESCs (data not shown). Based on these results, we decided to conduct a detailed analysis of the function of SOX17 using hESCs.

Sox17 promotes expansion of HE-like cells

SOX17 mRNA was highly expressed in EBs between days 2 and 4 of culture (Figure 1E). *SOX17* has been described as one of the master regulator genes for endodermal development.[10,22] High expression of *SOX17* in EBs at early time points supposedly reflects the development of endodermal cells. In contrast, ECs emerged at approximately day 6 in our culture system at the same time as increased expression of hematopoietic regulator genes such as *RUNX1* and *SCL/TAL1* (Figure 1C). Therefore, the expression of *SOX17* after day 6 may indicate a role of *SOX17* in hematopoietic development (Figure 1E). Indeed, *SOX17* was expressed at high levels in ECs, but at significantly lower levels in pre-HPCs, HPCs, and human CB $CD34^+$ cells (Figure 1F). Other *SOXF* family genes, *SOX7* and *SOX18*, showed a very similar pattern of expression profiles (Figure 1F).

To evaluate the effect of overexpression of *Sox17* in hematopoietic development in detail, we produced a retrovirus containing *Sox17* fused to *ERT* (*Sox17-ERT*). We transduced ECs from day 6 EBs with the *Sox17-ERT* retrovirus on OP9 stromal cells and cultured them in the presence of SCF and TPO. The addition of

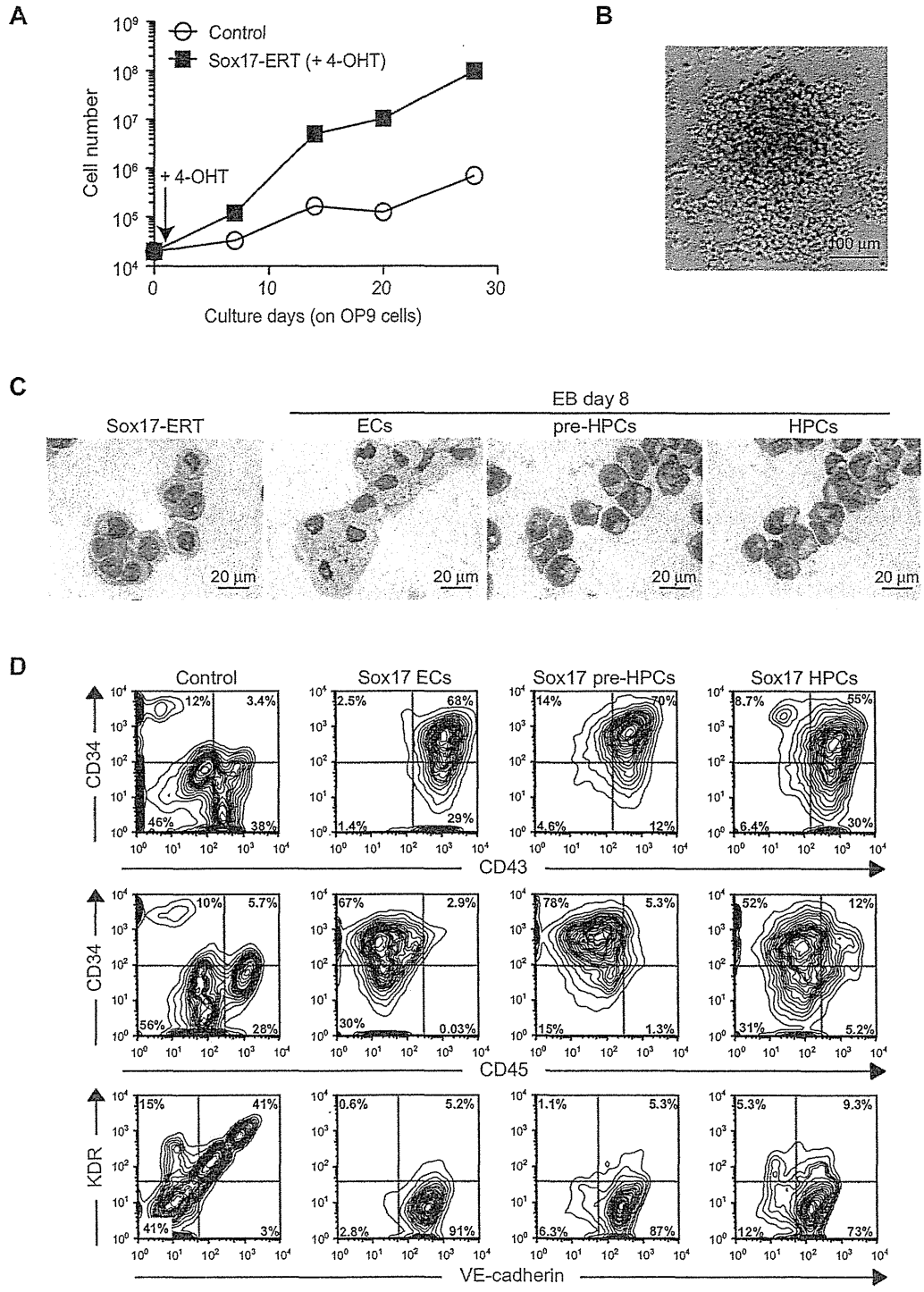

Figure 2. Sox17 promotes the expansion of CD34$^+$CD43$^+$CD45$^{-/low}$ cells. (A) Growth curve of ECs from day 6 EBs that were transduced with a *Sox17-ERT* or a control retrovirus. ECs (2×10^4) were transduced with the indicated retrovirus on OP9 cells and cultured in the presence of 20 ng/mL of SCF and TPO and 200nM 4-OHT. The absolute numbers of cells were determined and plotted. Representative data from repeated experiments are shown. (B) Appearance of a representative colony generated by *Sox17*-overexpressing cells in panel A observed under an inverted microscope. Images were collected using BIOREVO BZ-9000 (KEYENCE) with CFI Plan Fluor ELWD DM 20×C (Nikon). (C) Typical cell morphology of *Sox17*-overexpressing cells in panel A. Sorted cells were cytospun onto glass slides and observed after Wright-Giemsa staining. ECs, pre-HPCs, and HPCs from day 8 EBs served as controls. Images were collected using BIOREVO BZ-9000 (KEYENCE) with CFI Plan ApoVC 100×H (Nikon). (D) Flow cytometric analysis of expanded cells on overexpression of *Sox17*. ECs from day 6 EBs and pre-HPCs and HPCs from day 8 EBs were transduced with a *Sox17-ERT* or a control retrovirus cultured on OP9 in the presence of 20 ng/mL of SCF and TPO and 200nM 4-OHT for 10-15 days and then analyzed for their immunophenotypes.

4-OHT, which induces nuclear translocation of ERT fusion protein, considerably stimulated cell growth (Figure 2A). Overexpression of *Sox17-ERT* promoted cell growth moderately even without 4-OHT, suggesting leaky translocation of Sox17-ERT (data not shown). Indeed, Sox17-ERT was detected in both the nucleus and cytoplasm without 4-OHT, whereas the addition of 4-OHT induced

efficient nuclear translocation of Sox17-ERT (supplemental Figure 1A). *Sox17*-overexpressing cells formed semiadherent cell aggregates on OP9 cells (Figure 2B). Morphologic analysis revealed that they showed a monotonous morphology intermediate between ECs and pre-HPCs (Figure 2C). We performed further immunostaining with an anti-laminin Ab. After incubation in slide chambers for 4 hours, ECs attached to the slide glasses and stretched their cytoplasm out. In contrast, *Sox17*-overexpressing cells behaved like pre-HPCs and maintained a round shape, suggesting that *Sox17*-overexpressing cells do not retain strong adhesive properties of ECs, although they form semiadherent cell aggregates on OP9 cells (supplemental Figure 1B). Flow cytometric analysis demonstrated that *Sox17*-overexpressing cells expanded on OP9 cells were mostly $CD34^+CD43^+$ and did not express or expressed a low level of CD45 ($CD45^{-/low}$). These cells coexpressed the HE producer VE-cadherin (Figure 2D). Interestingly, overexpression of *Sox17* in pre-HPCs and HPCs from day 8 EBs similarly expanded $CD34^+CD43^+CD45^{-/low}$VE-cadherin$^+$ cells (Figure 2D). Although the endothelial-specific marker KDR/FLK1 was expressed in the majority of ECs from day 6 and 8 EBs (data not shown), its expression was immediately down-regulated during differentiation into pre-HPCs and HPCs and also on activation of Sox17 (Figure 2D).

Comprehensive gene-expression analyses using microarrays were performed to investigate the developmental stage of the cells expanded on overexpression of *Sox17*. ECs from day 6 and 8 EBs, pre-HPCs from day 8 EBs, and HPCs from day 8 and 12 EBs were transduced with *Sox17-ERT* and cultured on OP9 cells. These cells were then treated with 4-OHT and the resulting $CD34^+CD43^+CD45^{-/low}$ cells were subjected to microarray analysis. Freshly isolated ECs from day 6, 8, and 12 EBs, pre-HSCs from day 8 EBs, and HPCs from day 8 and 12 EBs served as control samples. The $CD34^+CD43^+CD45^{-/low}$ cells overexpressing *Sox17* appeared to express both EC-related genes such as *VE-cadherin/CDH5* and *ESAM* and hematopoietic-related genes such as *RUNX1* and *SCL/TAL1* (supplemental Table 1). Hierarchical clustering of the cell populations based on the microarray data of total genes revealed that *Sox17*-overexpressing cells showed very similar profiles of gene expression irrespective of the cell sources (ie, ECs, pre-HPCs, and HPCs; Figure 3A). We next performed clustering using probes corresponding to genes identified as "Transcription factor" and "Hemopoiesis" from the GO database. *Sox17*-overexpressing cells were developmentally placed between ECs and pre-HPCs/HPCs (Figure 3B-C). These findings, together with the intermediate morphology between ECs and pre-HPCs, suggest that $CD34^+CD43^+CD45^{-/low}$ cells expanded on the overexpression of *Sox17* are at a developmental stage between HE and early HPCs. To confirm this possibility, we then investigated whether the $CD34^+CD43^+CD45^{-/low}$ cells overexpressing *Sox17* give rise to mature hematopoietic cells on inactivation of Sox17 (Figure 4A). As expected, after depletion of 4-OHT, $CD34^+CD43^+CD45^{-/low}$ cells lost expression of CD34 and VE-cadherin but gained a higher level of CD45 expression and gave rise to $CD235a^+$ erythroblasts and $CD11b^+$ myeloid cells more efficiently than they did in the presence of 4-OHT (Figure 4B-C). This trend was confirmed in colony-forming assays. We seeded $CD34^+CD43^+CD45^{-/low}$ cells overexpressing *Sox17* in methylcellulose medium in the presence and absence of 4-OHT. *Sox17*-overexpressing cells in the presence of 4-OHT mainly formed compact colonies consisting of nonhemoglobinated cells with a morphology similar to ECs (Figure 2B), whereas they generated hemoglobinated erythroid colonies and myeloid colonies in the absence of 4-OHT (Figure 4D). These findings clearly indicate that the $CD34^+CD43^+CD45^{-/low}$ cells overexpressing *Sox17* still retain hemogenic potential, which becomes apparent on removal of 4-OHT.

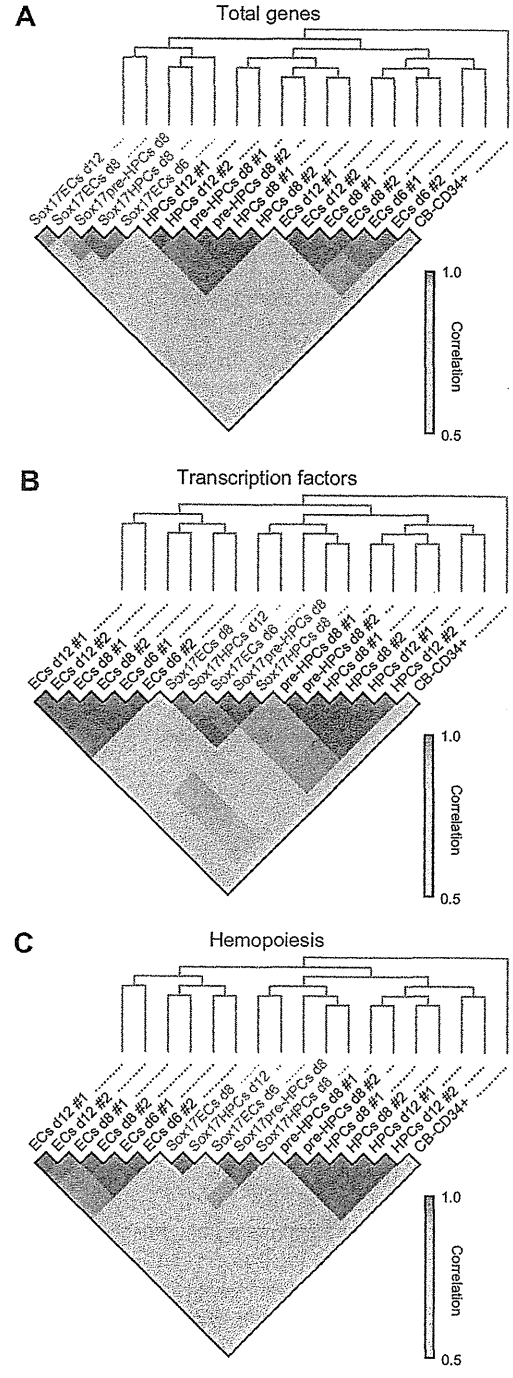

Figure 3. $CD34^+CD43^+CD45^{-/low}$ cells expanded on overexpression of *Sox17* developmentally place between ECs and pre-HPCs/HPCs. Gene-expression patterns of wild-type and *Sox17*-overexpressing cells obtained in microarray analyses were clustered using hierarchical clustering. The distance between 2 samples was defined with the Pearson correlation using total genes (A) or certain probes selected from the GO database (B-C). "Transcription factor" represents genes that are located in the nucleus and have at least 1 of the GO terms "regulation of transcription, DNA-dependent," "transcription factor activity," or "transcription factor complex" (B). "Hemopoiesis" represents genes that are annotated with the GO terms "hemopoiesis," "vasculogenesis," "erythrocyte differentiation," "erythrocyte maturation," and/or "erythrocyte development" (C). The color of each cell represents the value of correlation indicated on the right side of the matrix.

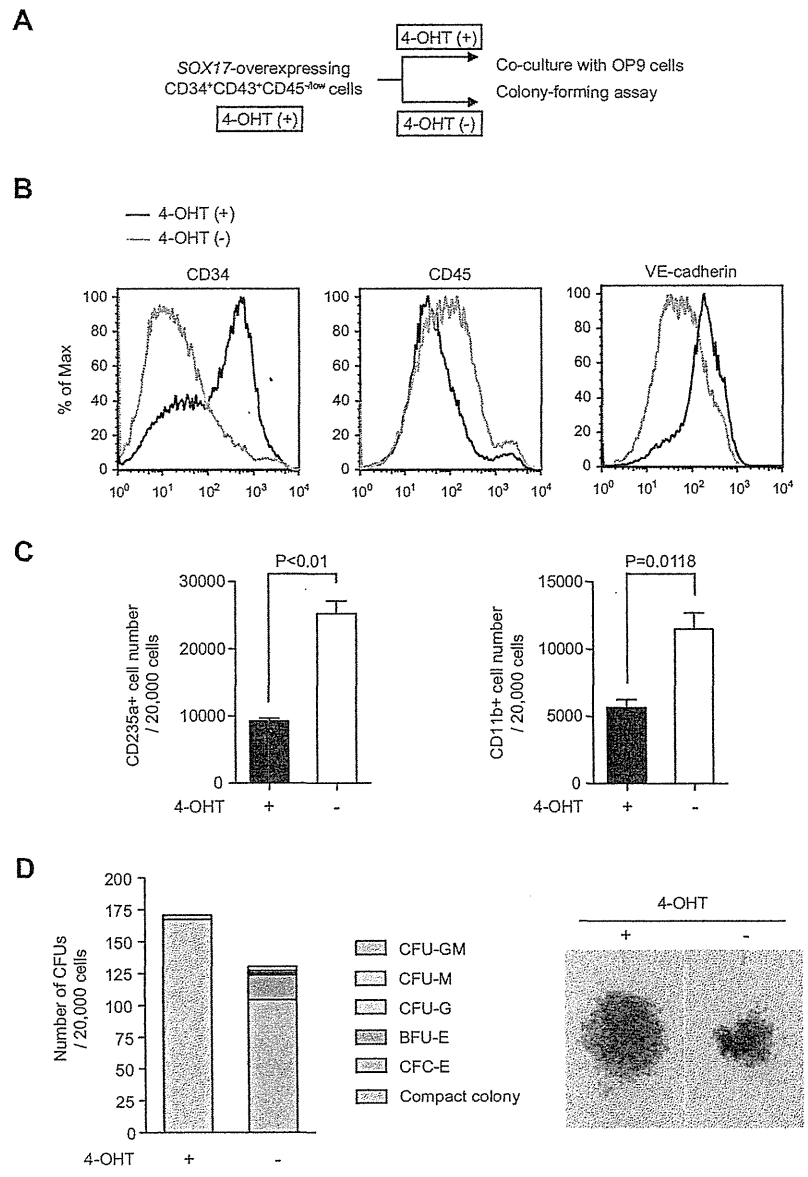

Figure 4. CD34$^+$CD43$^+$CD45$^{-/low}$ cells expanded on overexpression of *Sox17* retain hemogenic potential. (A) Experimental design to evaluate effects of withdrawal of 4-OHT on *Sox17*-overexpressing cells. ECs from day 6 EBs transduced with a *Sox17-ERT* retrovirus were cultured in the presence of 20 ng/mL of SCF and TPO and 200nM 4-OHT for 15 days. Then, the cells were subjected to coculture with OP9 cells and colony-forming assays. For coculture with OP9 cells, the cells were replated onto OP9 cells and cultured in the presence of 20 ng/mL of SCF and TPO, 10 ng/mL of IL-3, and 3 units/mL of erythropoietin with and without 4-oht. at day 7 of culture, the cells were analyzed for their immunophenotypes by Flow cytometry. For colony-forming assays, the cells were replated in methylcellulose in the presence of 20 ng/mL of SCF, 10 ng/mL of TPO and IL-3, and 3 units/mL erythropoietin with and without 4-OHT. At day 12 of culture, the colonies were counted. (B) Representative flow cytometric profiles of cells overexpressing *Sox17-ERT* before and after depletion of 4-OHT. (C) The absolute numbers of CD235$^+$ erythroblasts and CD11b$^+$ myeloid cells in culture at 7 days after depletion of 4-OHT. Data are shown as the means ± SD for triplicate cultures. (D) Ability of *Sox17-ERT*–overexpressing cells to form hematopoietic colonies in methylcellulose cultures with or without 4-OHT. The numbers of CFUs in culture are presented (left panel). CFU-GM, CFU-M, CFU-G, BFU-E, and CFU-E indicate CFU-granulocyte-macrophage, CFU-macrophage, CFU-granulocyte, burst-forming unit-erythroid, and colony-forming unit-erythroid, respectively. Compact colonies indicate colonies composed by HE cell–like cells. The appearance of a representative compact colony and an erythroid colony observed under an inverted microscope is depicted (right panel).

We next compared the expression of globin genes in *Sox17*-overexpressing CD34$^+$CD43$^+$CD45$^{-/low}$ HE-like cells and their hematopoietic progeny with globin gene expression in CB CD34$^+$ cells. CD34$^+$CD43$^+$CD45$^{-/low}$ cells expanded on overexpression of *Sox17* were further cultured in the presence and absence of 4-OHT for 7 days and then GFP$^+$ cells expressing *Sox17-ERT* were collected by cell sorting. RT-PCR analysis revealed that embryonic globin (ϵ) and fetal globin (γ), but not adult globin (β), were highly expressed in *Sox17*-overexpressing cells and/or their hematopoietic progeny (supplemental Figure 2). These results raise the possibility that the CD34$^+$CD43$^+$CD45$^{-/low}$ HE-like cells expanded on overexpression of *Sox17* are a hemogenic intermediate differentiated from hemangioblasts that primarily give rise to yolk sac–type blood cells.[8]

SOX17 is essential for the hemogenic activity of HE cells

Our results so far indicate that the overexpression of *Sox17* promotes the expansion of HE-like cells, but inhibits their hematopoietic differentiation into pre-HPCs. Because *SOX17* is highly expressed in ECs enriched in HE, we examined the role of SOX17 by knock-down analysis. We transduced ECs from day 5 EBs with lentiviruses expressing shRNA against *SOX17* on OP9 cells and allowed them to differentiate into hematopoietic cells for 9 days. The most effective shRNA, sh-*SOX17*#1273 (Figure 5A), suppressed the development and differentiation of hematopoietic cells including both erythroblasts and myeloid cells significantly, whereas it only moderately diminished the growth of CD235a$^-$CD11b$^-$ nonhematopoietic cells, the majority of which do not express SOX17 even though approximately 25%-30% of these cells are SOX17$^+$ ECs (Figure 5B-C). sh-*SOX17*#1143 similarly, albeit modestly, suppressed the production of hematopoietic cells. Similar results were obtained when we knocked down *SOX17* in ECs from day 6 EBs (data not shown). However, hematopoietic differentiation was not affected on *SOX17* knock-down in pre-HPCs from day 8 EBs (Figure 5D). These findings indicate that SOX17 plays a key role in the acquisition of hematopoietic potential in HE cells.

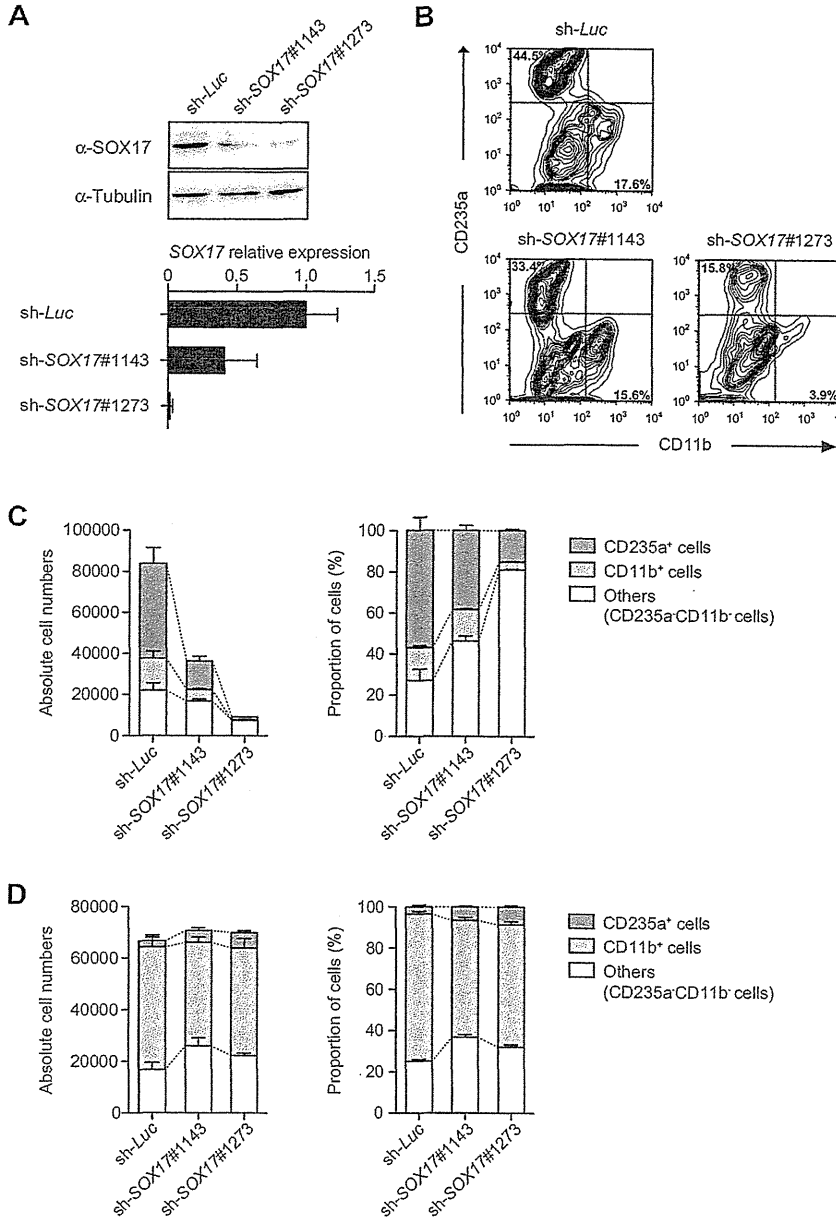

Figure 5. Hematopoietic differentiation from HE is inhibited by depletion of SOX17. (A) Knock-down efficiencies of shRNAs against *SOX17*. Western blot analysis of SOX17 in 293T cells transduced with shRNAs against *SOX17* (top panel). α-Tubulin was used as the loading control. pre-HPCs from day 8 EBs were transduced with shRNAs against *SOX17* on OP9 cells and cultured in the presence of 20 ng/mL of SCF and TPO, 10 ng/mL of IL-3, and 3 units/mL of erythropoietin (EPO) for 7 days. Levels of endogenous *SOX17* were analyzed by quantitative RT-PCR analysis (bottom panel). mRNA levels were normalized to *GAPDH* expression. Expression levels relative to that in the control cells transduced with an shRNA against *Luciferase* are shown as the means ± SD for triplicate analyses. (B) Effects of depletion of SOX17 on hematopoietic development from HE cells. ECs from day 5 EBs were transduced with shRNAs against *SOX17* on OP9 cells and were cultured in the presence of 20 ng/mL of SCF and TPO, 10 ng/mL of IL-3, and 3 units/mL of EPO for 9 days. Representative flow cytometric profiles of cells at day 9 of culture are depicted. (C) Absolute numbers and proportion of CD235a$^+$ erythroblasts and CD11b$^+$ myeloid cells in panel B at day 9 of culture. Data are shown as the means ± SD for 3 independent cultures. (D) Effects of depletion of SOX17 on pre-HPCs. Pre-HPCs from day 8 EBs were transduced with shRNAs against *SOX17* on OP9 cells and were cultured in the presence of 20 ng/mL of SCF and TPO, 10 ng/mL of IL-3, and 3 units/mL of EPO for 7 days. Absolute numbers and proportion of CD235a$^+$ erythroblasts and CD11b$^+$ myeloid cells at day 7 of culture are presented. Data are shown as the means ± SD for triplicate cultures of 1 of 2 independent experiments that gave similar results.

SOX17 regulates directly the transcription of key regulator genes for HE cells

A ChIP-on-chip analysis was conducted to identify the direct target genes of SOX17 in HE cells. We transduced ECs cells from day 6 EBs with a *3xFlag-Sox17-ERT* retrovirus and expanded CD34$^+$CD43$^+$CD45$^{-/low}$ HE-like cells on OP9 cells. At day 27 of culture, 94.2% of the expanded cells were positive for CD34. CD34$^+$ cells were further enriched (99.8%) by magnetic cell sorting using magnetic beads conjugated with anti-CD34 Abs, and these purified cells were then subjected to ChIP-on-chip analysis.

The ChIP-on-chip analysis was performed with human promoter microarrays containing approximately 21 000 probe sets covering from −8.0 kb upstream to +4.0 kb downstream of the TSS of RefSeq genes. 3xFlag-Sox17 was cross-linked to DNA and precipitated using the anti-FLAG M2 Ab. Gene promoters bound by Sox17 were ranked according to fold enrichments calculated in comparison with signals obtained with the input DNA. Of the 19 457 gene promoter regions analyzed, 182 and 98 regions showed Sox17 binding with an enrichment greater than 2- and 3-fold, respectively (full data are listed in supplemental Table 2). The functional annotation of the genes bound by Sox17 with a fold enrichment greater than 3 was performed based on GO and showed significant enrichment for genes that fell into categories such as "vasculogenesis," "hemopoiesis," and "positive regulation of erythrocyte differentiation" (Figure 6A, Table 1, and supplemental Table 2). The genes bound by Sox17 include genes well characterized as regulators of hematopoietic development from HE cells, such as *VE-cadherin/CDH5*, *RUNX1*, *SCL/TAL1*, and *HHEX* (Table 1 and supplemental Table 2). VE-cadherin, an endothelial marker antigen, is expressed by HE cells and by early HSCs, which appear in the yolk sac and the aorta-gonad-mesonephros region, as well as by a transient HSC population of the fetal liver.[23-25] *RUNX1*, *SCL/TAL1*, and *HHEX* encode transcription factors essential for the development of HSCs from HE cells or hemangioblasts.[5,26,27] The

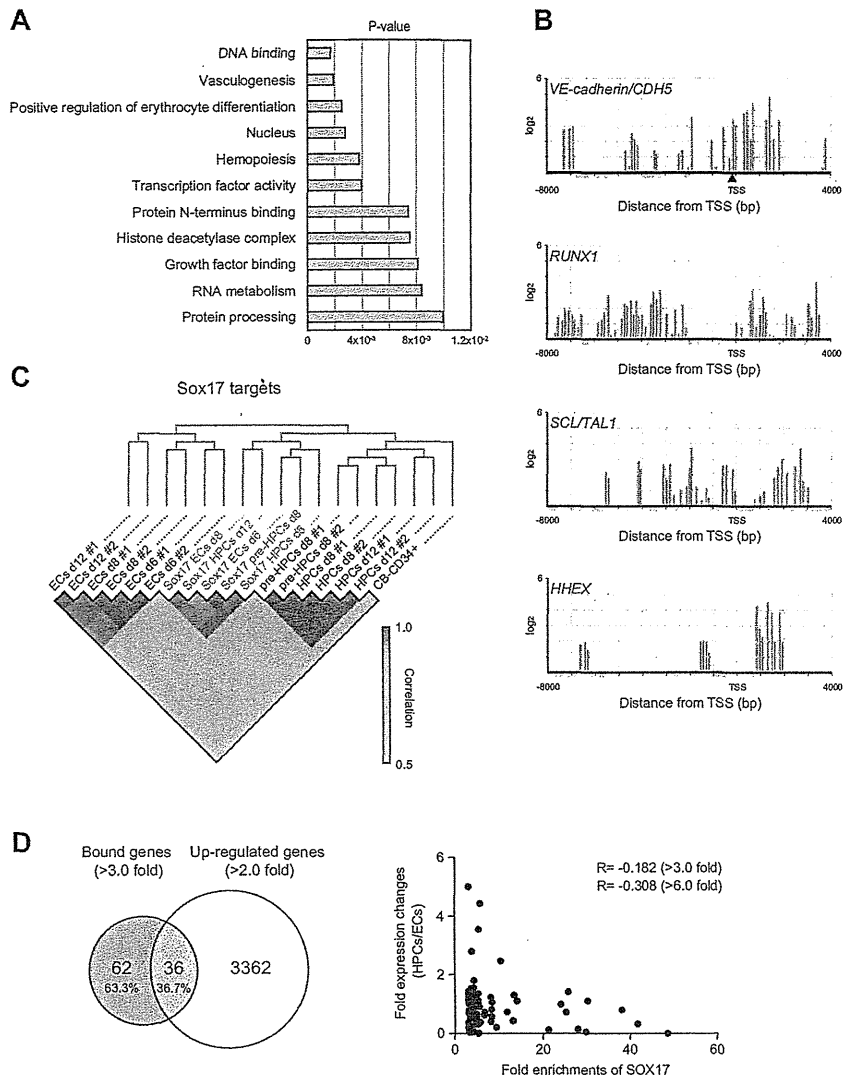

Figure 6. Targets of SOX17 detected by ChIP-on-chip analysis. (A) GO analysis of the Sox17 targets detected by ChIP-on-chip analysis. $CD34^+CD43^-$ cells from day 6 EBs were transduced with a 3× Flag *SOX17-ERT* retrovirus. The cells were further cultured on OP9 cells in the presence of 20 ng/mL of SCF and TPO and 200nM 4-OHT. $CD34^+$ cells were collected at day 27 of culture and subjected to ChIP-on-chip analysis. *P* for each GO term is indicated. (B) ChIP-on-chip profile of SOX17 occupancy at genes related to hematopoietic development from HE cells. Plot under the x-axis shows the position of probe sets. Arrowhead at the *VE-cadherin/CDH5* promoter indicate consensus motif of Sox17-binding site. (C) Gene-expression patterns of wild-type and engineered cells obtained in microarray analyses clustered using hierarchical clustering. Distance between 2 samples was defined with the Pearson correlation of Sox17 target genes with Sox17 binding more than 3-fold in the ChIP-on-chip analysis presented in supplemental Table 2. The color of each cell represents the value of correlation indicated on the right side of the matrix. (D) Comparative analysis of ChIP-on-chip and microarray data. Venn diagrams showing the number of genes bound by Sox17 (> 3-fold enrichment) and the number of genes up-regulated in expression more than 2-fold in at least 1 cell type among ECs, pre-HPCs, and HPCs on overexpression of *Sox17* (*Sox17*-overexpressing $CD34^+CD43^+CD45^{-/low}$ cells compared with those of respective fresh controls; left panel). The percentages of overlapping and nonoverlapping bound genes are indicated in parentheses. Shown are the correlation of Sox17 binding (fold enrichment) in ChIP-on-chip analysis and the fold changes in expression during differentiation of ECs to HPCs (right panel). The fold enrichments and fold changes in expression were plotted for 84 genes of 98 showing enrichments greater than 3-fold (the microarray data were not available for the remaining 14 genes). Correlation coefficients (R) are indicated for genes with fold enrichment greater than 3- and 6-fold, respectively.

distribution of SOX17 signals at these genes varied greatly across the promoter region (Figure 6B). SOX17 is reported to bind to the consensus motif of "ATTGT."[22] The *VE-cadherin/CDH5* promoter contains the consensus motif between −107 bp and −103 bp from the TSS. It was recently reported that this site is conserved in mouse and Sox7 binds directly to it to activate transcription.[28] Our ChIP-on-chip data showed that Sox17 binds to this site as well (Figure 6B arrowhead). These findings clearly indicate that SOX17 regulates directly the expression of a set of key genes for hematopoietic development in HE cells.

We next performed hierarchical clustering of the cell populations based on the microarray data using "SOX17 targets" that we arbitrarily selected as genes with Sox17 binding greater than 3-fold over the input levels in the ChIP-on-chip analysis (supplemental Table 2). As expected, *Sox17*-overexpressing cells were again developmentally placed between ECs and pre-HPCs/HPCs (Figure 6C).

Comparison of gene lists between the ChIP-on-chip and microarray assays

We next examined the changes in expression of the 98 genes bound by Sox17 (> 3-fold enrichment in the ChIP-on-chip analysis) on *Sox17* overexpression. The microarray data of *Sox17*-overexpressing $CD34^+CD43^+CD45^{-/low}$ cells shown in Figure 3 were compared with those of respective fresh controls. Sox17 is thought to activate the transcription of target genes.[22] As expected, 36 of the 98 genes showed up-regulation in expression of more than 2-fold in at least in 1 cell type (Figure 6D, Table 1, and supplemental Table 2). This tendency was evident in the top 15 genes with Sox17 binding (Table 1 and supplemental Table 2), although in 4 genes of 15, the effects of overexpression of *Sox17* were obvious only in pre-HPCs and HPCs, but not in ECs, which possess a high level of endogenous SOX17 (supplemental Table 2). Similarly, a negative correlation was detected between the levels of Sox17 binding in ChIP-on-chip analysis and the fold changes in expression during differentiation of ECs ($SOX17^+$) to HPCs ($SOX17^-$; Figure 6D). Among genes bound by Sox17, *EGFL7* and *VE-cadherin/CDH5* have been shown to be up-regulated in BM HPCs transduced with *Sox17*.[13] However, in our ChIP-on-chip analysis, Sox17 did not show any binding to the genes directly regulated by Sox17 during differentiation of ES cells into extraembryonic endoderm.[22] These data suggest that SOX17 regulates different targets in hematopoietic and endodermal development.

Table 1. Candidate SOX17 target genes according to ChIP-chip scores

				GO term			Fold difference		
Rank	Symbol	Gene name	Fold enrichment	Vasculogenesis	Positive regulation of erythrocyte differentiation	Hemopoiesis	Sox17 ECs d6/ECs d6	Sox17 pre-HPCs d8/pre-HPCs d8	Sox17 HPCs d8/HPCs d8
1	GPSM3	G-protein signaling modulator 3	48.50	No	No	No	1.38	2.42	2.56
2	MAST4	Microtubule associated serine/threonine kinase family member 4	41.62	No	No	No	1.02	3.22	4.75
3	TXLNB	Taxilin beta, muscle-derived protein 77	38.05	No	No	No	1.18	2.89	4.29
4	EGOT	Eosinophil granule ontogeny transcript	37.53	No	No	No	ND	ND	ND
5	PPBPL1	Pro-platelet basic protein-like 1	35.26	No	No	No	ND	ND	ND
6	MFSD6	Major facilitator superfamily domain containing 6	30.27	No	No	No	19.79	14.24	19.26
7	CDH5	Cadherin 5, type 2	29.86	No	No	No	0.70	9.07	10.81
8	BCL6B	B-cell CLL/lymphoma 6, member B	28.05	No	No	No	1.11	5.73	8.50
9	C1orf55	Chromosome 1 open reading frame 55	25.81	No	No	No	2.23	1.77	1.44
10	PTTG1IP	Pituitary tumor-transforming 1 interacting protein	25.28	No	No	No	0.93	1.49	1.67
11	TRIM67	Tripartite motif containing 67	24.08	No	No	No	4.16	4.29	5.03
12	MYCT1	myc target 1myc target 1	21.26	No	No	No	0.74	2.90	7.66
13	CD40LG	CD40 ligand	14.12	No	No	No	6.65	11.57	16.69
14	SCOC	Short coiled-coil protein	13.45	No	No	No	0.97	0.79	1.04
15	PPP1R16B	Protein phosphatase 1, regulatory subunit 16B	13.18	No	No	No	0.70	1.83	1.15
19	ACVR2A	Activin A receptor, type IIA	9.45	No	Yes	No	0.15	0.42	0.67
26	HHEX	Hematopoietically expressed homeobox	6.87	Yes	No	Yes	0.66	1.44	0.89
37	RUNX1	runt-related transcription factor 1	5.46	No	No	Yes	5.02	1.25	1.12
41	TAL1/SCL	T-cell acute lymphocytic leukemia 1	5.28	No	Yes	Yes	1.82	1.76	1.92
50	EGFL7	EGF-like-domain, multiple 7	4.69	Yes	No	No	0.67	2.11	1.92
69	JUNB	jun B protooncogene	3.78	Yes	No	No	3.50	3.87	3.24

ND indicates no data.